Journal of Structural Geology 31 (2009) 270–287

Contents lists available at ScienceDirect

Journal of Structural Geology

journal homepage: www.elsevier.com/locate/jsg

The relationship between forceful and passive emplacement: The interplay between tectonic strain and magma supply in the Rosses Granitic Complex, NW Ireland

Carl Stevenson*

School of Geography, Earth and Environmental Sciences, University of Birmingham, Edgbaston, Birmingham, West Midlands B15 2TT, UK

ARTICLE INFO

Article history:
Received 2 July 2008
Received in revised form
14 November 2008
Accepted 24 November 2008
Available online 6 December 2008

Keywords:
Forceful and passive emplacement
Shear zone
Rosses Granite Complex
Donegal Batholith
AMS

ABSTRACT

The Rosses Granitic Complex, NW Ireland, part of the late Caledonian (c. 400 Ma) Donegal Batholith, provides the opportunity to study the interplay between relative tectonic strain and magma supply rates in the wall of a major tectonic shear zone. Anisotropy of magnetic susceptibility (AMS) measurements, structural analysis and examination of key intrusive relationships were used to assess the accommodation of magma, associated deformation and magma flow pathways in this complex. In this case the varying emplacement styles, switching from forceful to passive, indicate that relative tectonic strain and magma supply rates were not constant. In the earliest component (a suite of microgranite sheets), AMS reveals subtle fabrics discordant to the sheet margins and is interpreted as post-emplacement deformation fabrics. The concordance of these fabrics to the next component of the complex, the main pluton (G1 and G2 monzogranite), indicates that this deformation was caused by the forceful emplacement of the pluton. AMS fabrics in G1 and G2 reveal a dome shaped foliation with an east-west lineation, indicating an east-west oriented magma transport direction. Outcrops of small stocks or cupolas similar to G2, east of the main pluton, link it to similar lithologies in the Main Donegal Granite further to the east via a partially exposed lateral feeder. This suggests east to west emplacement. The next component, a suite of subvertical porphyritic felsite dykes, is shown (from AMS and visible shearing fabrics) to have been emplaced passively under east-west tension. The final component comprises G3 and G4 of the main pluton, which passively cut all earlier components and contains significant amounts of aplite, pegmatite and greisen. These are interpreted to be cupolas or stocks emanating from an unexposed sheet probably similar in composition and mode of emplacement to G1 and G2. Thus, a general model is put forward where initially forceful subhorizontal sheets extending laterally from the nearby Main Donegal Granite shear zone, gave way to passive emplacement where the roofs of these and subjacent sheets failed. The control on siting of the complex can be related to lower crustal structures, which control upper crustal shear zones. The reason for the switch in emplacement style is suggested to be due to a waning magma supply, in a tectonic strain field where the extensional component was oriented east-west. The waning magma supply then possibly due to switching of the site of emplacement of magma, supplied by the Main Donegal Granite shear zone, to another member of the Donegal Batholith – the Trawenagh Bay Granite.

1. Introduction

The tectonic control of the ascent and emplacement of granitic magma in high strain zones is well established (e.g. Brun and Pons, 1981; Hutton, 1982, 1988a,b, 1992, 1996; Reavy, 1989; Hutton and Reavy, 1992; McCaffrey, 1992; Ingram and Hutton, 1994; Hutton and Alsop, 1996; Jacques and Reavy, 1996; Mahan et al., 2003). Forceful emplacement occurs when magma supply exceeds the rate of space creation achieved by tectonic deformation (tectonic opening) and magma is therefore required to shoulder aside the country rocks. Whereas passive emplacement occurs when opening rates are great enough in comparison to magma supply rates that magma fills the space passively with no shouldering aside (Hutton, 1988b). An alternative passive emplacement mechanism that requires no tectonic space creation is cauldron subsidence, where a large block of country rock has subsided passively into a subjacent magma chamber and the space vacated by the block filled with upwelling magma from the subjacent chamber (Richey, 1928, 1932; Cole et al., 2005). In low strain zones, it is also now well established that granite plutons form tabular shaped bodies constructed from

* Tel.: +44 121 414 6136; fax: +44 121 414 4942.
E-mail address: c.t.stevenson@bham.ac.uk

0191-8141/$ – see front matter © 2008 Elsevier Ltd. All rights reserved.
doi:10.1016/j.jsg.2008.11.009

vertically thickened subhorizontal sheets – essentially laccoliths (Cruden, 1998; McCaffrey and Petford, 1997; Petford and Clemens, 2000; Cruden and McCaffrey, 2001), see Petford et al. (2000) and Vigneresse (2005) for discussion on ascent and emplacement of granitic magma. In this case, tectonic strain is effectively zero and emplacement is forceful. However, the link between ascent through a high strain zone and emplacement outside this zone is poorly understood, especially when there is potentially both forceful and passive emplacement operating.

The late Caledonian (~400 Ma) Donegal Batholith (Fig. 1) displays a range of forceful and passive emplacement styles penecontemporaneously, and in the wall of a major tectonic shear zone (Hutton, 1982; Price, 1997), which potentially provided the deeply penetrating ascent route for the magma (Stevenson et al., 2008). This situation provides the ideal opportunity to study the relationship between forceful and passive emplacement in the upper crust (Pitcher and Berger, 1972), set against a batholithic ascent and emplacement model (Stevenson et al., 2008).

The Rosses Complex, one of the younger members of the Donegal Batholith, is made up of a series of microgranite sheets, a swarm of porphyritic felsite dykes and the Rosses granite pluton (Fig. 2) (Pitcher and Berger, 1972). Pitcher (1953a) described the structure and petrology of this complex concluding that it represented an example of the cauldron subsidence mechanism. This passive emplacement mechanism was set against the closely associated (spatially and temporally) forceful emplacements of the Ardara and Main Donegal Granite plutons by Pitcher and Berger (1972).

This study uses anisotropy of magnetic susceptibility (AMS) measurements to examine the fabrics in the constituent intrusions of the Rosses Complex. Key field relationships are also examined and together with the fabric data, the accepted fracture controlled cauldron subsidence model is critically evaluated and a new model involving an initial phase of lateral emplacement and vertical thickening and doming is proposed. This new model is set against the emplacement of the Main Donegal Granite (Hutton, 1982) and the Donegal Batholith (Stevenson et al., 2008) and the implications for predicting mineralisation discussed.

1.1. The geology of the Rosses Complex: fracture controlled cauldron subsidence

The identification of steep cross cutting contacts led Pitcher (1953a) to interpret the Rosses Pluton as an example of cauldron subsidence. He suggested that the concentric but weak fabrics supported a passive emplacement model and that the polygonal pattern of the G2–G3 contact held the key to the emplacement mechanism of the whole pluton; that the contacts followed pre-existing joint sets. The significant feature of Pitcher's (1953a) model was the apparent control of the contact orientations by fracture

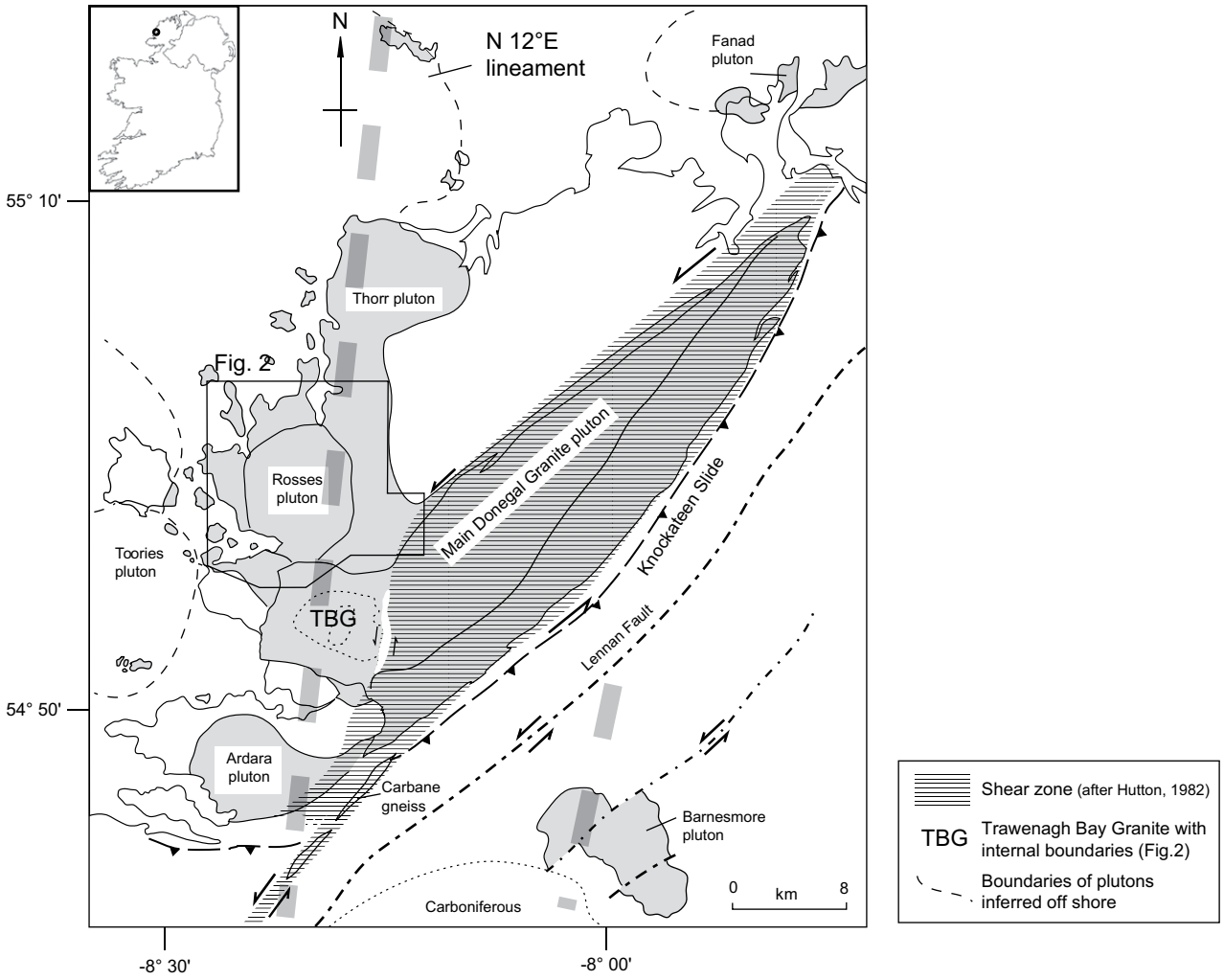

Fig. 1. The plutons of the Donegal Batholith modified after Pitcher and Berger (1972). The extent of the Main Donegal Granite shear zone is taken from Hutton (1982) and the position of the N12°E from Hutton and Alsop (1996).

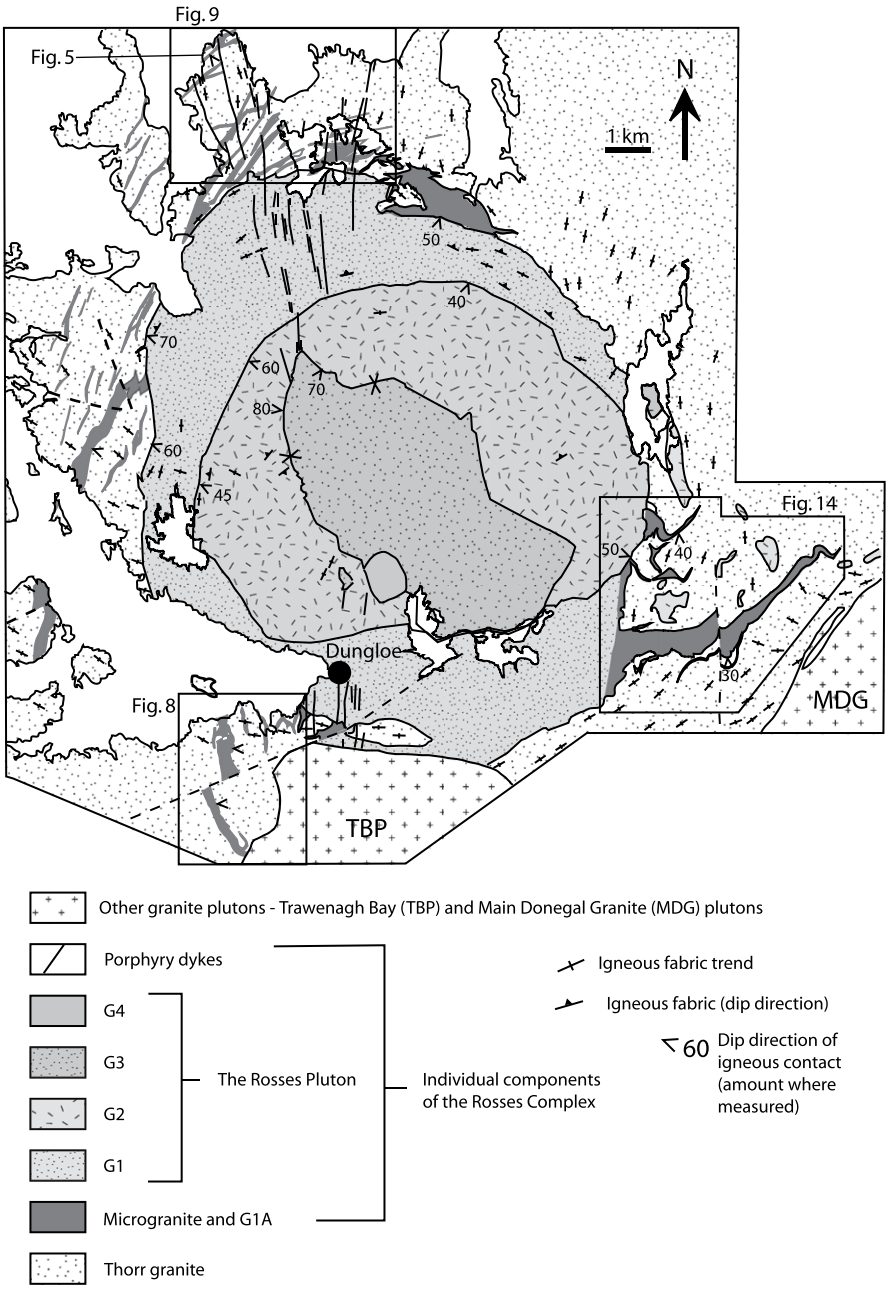

Fig. 2. The geology of the Rosses area modified after Pitcher (1953a). The metasedimentary xenoliths of the Thorr Pluton are omitted.

sets, where upward directed magma pressure exploited pre-existing fractures or 'master joints' rather than instigating a new ring-fault/dyke (Read, 1958); a modification of Anderson's (1936) ring-dyke mechanism. Subsequent to Pitcher's (1953a) work, pre-existing fracture controlled cauldron subsidence was established as an important emplacement mechanism in the Peruvian Coastal Batholith (Bussell et al., 1976; Cobbing et al., 1981; Cobbing and Pitcher, et al., 1985; Pitcher, 1997, p. 202–246, 242; Bussell and Pitcher, 1985; Haederle and Atherton, 2002) and elsewhere (e.g. Dehls et al., 1998; Lacroix et al., 1998; Chernicoff et al., 2002). The Rosses Complex was thus a seminal study for the Peruvian Coastal Batholith model and remains an important example of cauldron subsidence and fracture controlled magma emplacement (see Hall, 1966, p. 81; Pitcher, 1997, p. 202; Pitcher and Hutton, 2004, p. 60).

Hall (1966) suggested that the microgranite sheets represented the initial fracturing of the roof of a magma chamber in the cauldron subsidence emplacement model. He also postulated that the partially radial disposition of the porphyry dykes was due to inflation of an underlying magma chamber modified by east-west tensional stresses. This has important implications in terms of understanding the timing and circulation of mineralising fluids, as only the latest stages of the Rosses exhibit mineralisation (Pitcher, 1953a).

The petrology and the field relations of the various constituent parts of the Rosses Complex were studied in detail by Pitcher (1953a,b), Mercy (1962) and Hall (1966). The Rosses Pluton consists of relatively homogeneous biotite–muscovite monzogranite with a roughly circular outcrop, ~8.5 km in diameter emplaced entirely into the Thorr Pluton (Pitcher, 1953a,b) (Fig. 2). Pitcher (1953a) identified four separate, roughly concentric, units (G1–G4) in the pluton. These separate units were identified based mainly on the variation of grain size and delineated by sharp but discontinuous contacts sometimes characterised by accumulations of pegmatite

or aplite. The G1 unit also contains a marginal G1A facies, which is essentially a finer grained variant of G1 and exhibits both transitional and cross cutting boundaries with some large microgranite sheets.

Pitcher (1953a) measured very weak fabrics in the Rosses Pluton, defined by biotite, in orientated thin sections of samples from G1 and G2. These fabrics were generally parallel with the contacts and, due to a lack of evidence for plastic deformation, of magmatic-state (Fig. 2).

The microgranite sheets are younger than the pluton and crop out within ~3–4 km around the periphery in three main areas; around the northwest, in the east and a small area in the southwest. Pitcher (1953a) described a range of microgranite sheets; a dark biotite rich variant, a pale biotite rich variant, a pale muscovite rich variant and a coarser porphyritic variant. Generally, the darker biotite rich variety is earliest and is usually cut by the paler sheets. In the east, three large microgranite sheets dip moderately north, strike at a high angle to the margins of the pluton and are up to ~70 m thickness. A significant feature of the largest sheet at Crovehy (also present in the Pollcrovehy sheet) is its xenolith–strewn base or floor (near the southern contact). According to Pitcher (1953a), the xenolith rich portion of these sheets appears to be continuous with the G1A facies that fringes the Rosses G1 in some eastern marginal areas (Fig. 2). Fabrics in these sheets are also very weak.

The porphyry dykes are feldspar- and biotite-pheric felsites. These dykes intrude the Rosses G1 and G2 units but are then cut by the Rosses G3 unit.

Parts of the G3 unit and the whole G4 unit are characterised by areas of greisen and greisen veins. Pitcher (1953a) suggested that the same joint pattern that controlled the emplacement of these last two units facilitated the circulation of late fluids.

Pitcher (1953a,b) described a number of enigmatic isolated outcrops of coarse grained quartz rich granite occurring in the area to the east of the pluton around the large microgranite sheets in this area (Fig. 2). These coarse bodies are similar to the coarse granite of the G2 unit in the Rosses Pluton.

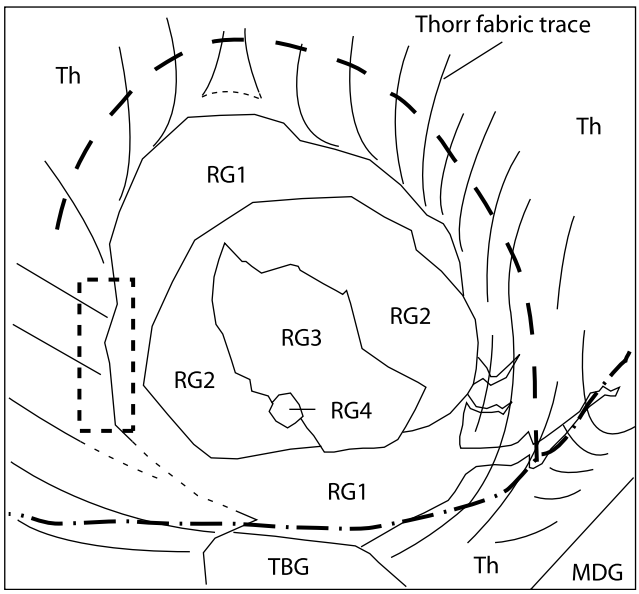

Fig. 3. Summary of the fabric trends in the Thorr Pluton and the contacts of the Rosses Pluton. The limit of deflection of Thorr fabrics close to the Rosses Pluton is highlighted with a dashed line. The limit of deflection of fabrics in the Main Donegal shear zone is highlighted with a dashed and dotted line. The latter may involve a combination of both of these strain fields and results in a tricuspid interference pattern in the southeast of the figure. Only in a small area along the western contact of the Rosses Pluton (highlighted with a dashed box) are Thorr fabrics truncated at a high angle in a similar way to the Trawenagh Bay Granite western contact to the south. Th – Thorr Pluton; TBG – Trawenagh Bay Granite; MDG – Main Donegal Granite, RG1, 2, etc. – Rosses Granite G1, G2, etc.

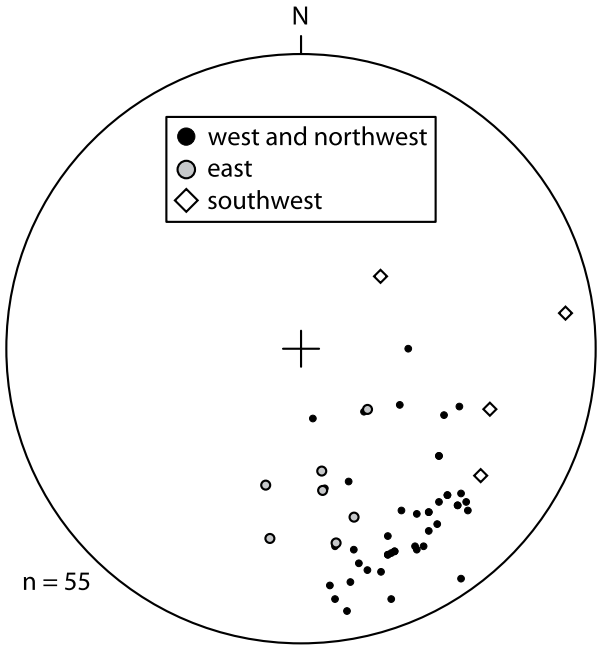

Fig. 4. Stereographic projection showing the orientation of the microgranite sheets in the three main areas.

2. Structural observations: new visible fabric data, field relations and contact geometries

2.1. The Rosses Pluton

No new visible fabrics in the Rosses Pluton can be added to the observations of Pitcher (1953a). The only new fabrics are those revealed by AMS analysis described below.

2.2. The Thorr Pluton

Although Pitcher (1953a) noted that the fabrics in the Thorr Pluton were cut by the Rosses Pluton and are thus not related to its emplacement, it is pointed out here that this is not generally true.

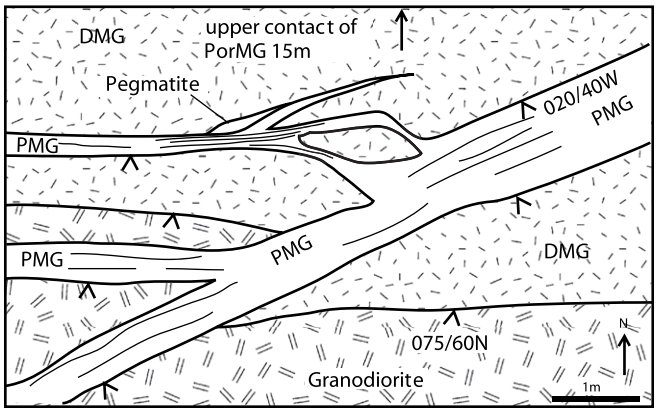

Fig. 5. Sketch map of the contact relations of a dark microgranite sheet (DMG) cut by a pale microgranite sheet (PMG) (see Fig. 2 for location). Both of these intrude Thorr granodiorite. Thin lines represent faint banding in the PMG. The offset of the DMG contact across the PMG sheets is in a reverse sense. The strike/dip and dip direction is noted for some contacts.

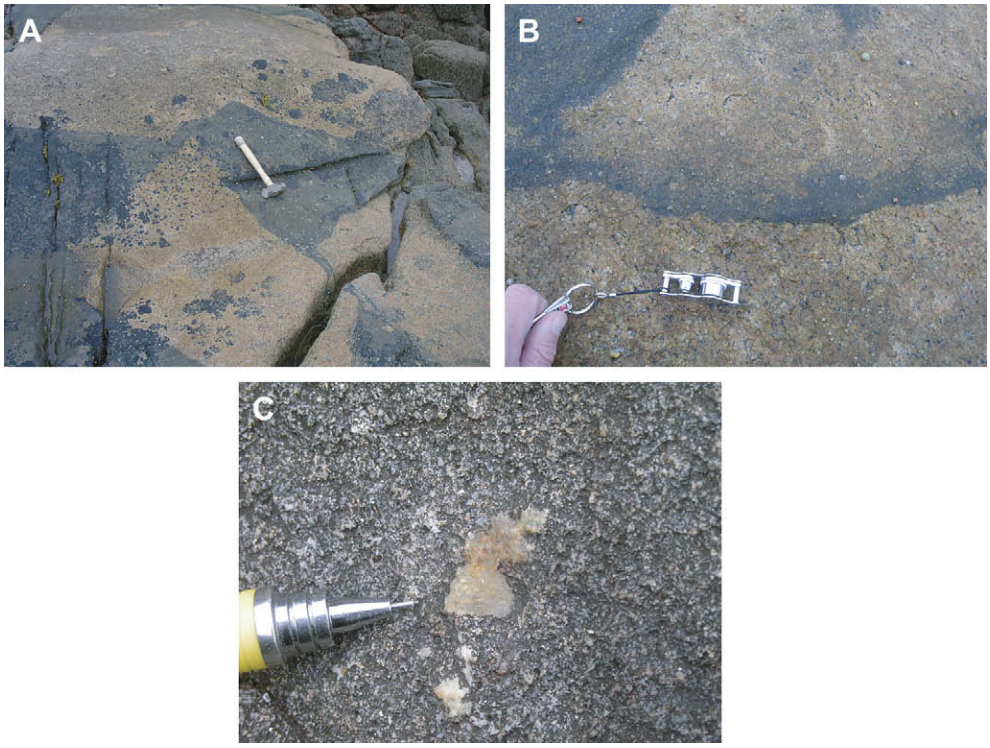

Fig. 6. (A) Photograph of a dark microgranite sheet, containing angular blocks of Thorr granodiorite. In detail, the margins are rounded–subrounded. (B) Close up of the margins of two of the granodiorite xenoliths showing the variation between sharp cross cutting (of the lower xenolith) and lobate and diffuse relationships (of the upper xenolith). Xenocrysts of Thorr feldspar are seen in the dark microgranite. (C) Close up of a xenocryst of feldspar in the microgranite. Note the irregular embayed contacts of the xenocryst.

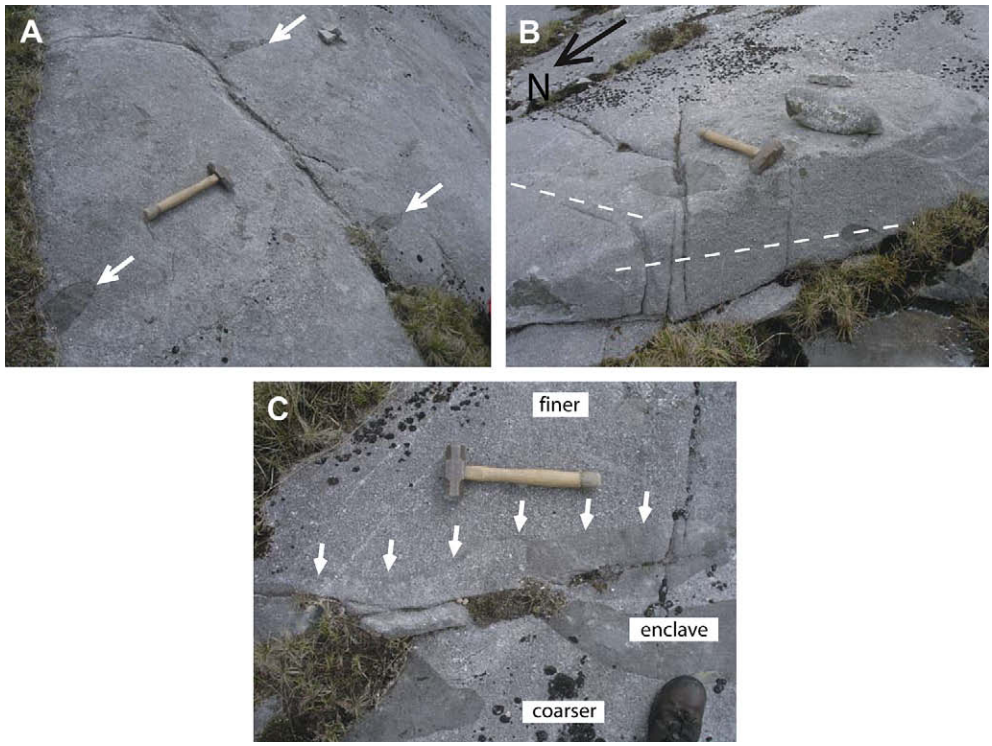

Fig. 7. (A) Field photograph of an outcrop of microgranite from the Crovehy Sheet showing enclaves of a more biotite rich microgranite (highlighted with white arrows) elongated roughly east-west (parallel with the hammer). (B) Field photograph of an outcrop of microgranite (roughly the same locality as A). Enclaves in this outcrop are flattened in a subhorizontal plane and elongated roughly east-west (parallel with the hammer). (C) Field photograph of microgranite (same locality) showing an internal contact (marked by white arrows) between a slightly coarser microgranite (pale) and a finer microgranite (darker). An enclave in the paler microgranite is truncated by the darker microgranite. This contact trends roughly east-west.

In Fig. 2, from Pitcher's own data, Thorr fabrics in the east and southeast of the Rosses Pluton are disposed roughly parallel to the Rosses Pluton contacts and fabrics in the northeast and northwest swing into at least partial parallelism with it (Fig. 3). Only in one small area on the western margin are Thorr fabrics truncated by the Rosses Pluton at a high angle. This is similar to the western contact of the Trawenagh Bay Granite western contact (Stevenson et al., 2007a). The microgranites usually cross cut Thorr magmatic- and solid-state fabrics. Liquid–liquid relationships between Thorr and microgranites are also found (see below).

2.3. The microgranite sheets

The microgranite sheets in the northwest are usually between 1 and 20 m thickness, strike NNW to NE (approximately tangential to the margins of the Rosses Pluton) and always dip away from the Rosses centre, although the amount of dip varies between 20 and 85° (Fig. 4). Fabrics in the northwest microgranite sheets usually strike very roughly parallel with the margins of the sheets and dip in the same direction but more steeply. These fabrics also seem to be more consistently parallel with the margins of the Rosses Pluton than the microgranite sheets. The pale microgranite sheets sometimes exhibit contact parallel banding and when they cut darker sheets, they usually offset these sheets in a reverse sense (Fig. 5).

Xenoliths or enclaves are rare in the northwest sheets. However, xenoliths of Thorr tonalite have been discovered north of Kincasslough at 55°2′18″N, 8°23′W in dark microgranite sheets (Fig. 6). These xenoliths are up to ~1 m in size and display a variety of contact relationships from sharp angular to lobate to gradational, even on the same xenolith. There are also plagioclase xenocrysts (displaying embayed margins) in the microgranite most likely derived from the host tonalite. The significance of these observations will be discussed below.

The eastern microgranite sheets contain biotite rich and muscovite rich variants. The largest sheet at Crovehy contains all variants and the sheet at Pollcrovehy contains mainly muscovite rich microgranite. The northernmost sheet, Lettercau, has again both biotite and muscovite rich variants. These sheets dip 20–40° north (Fig. 4).

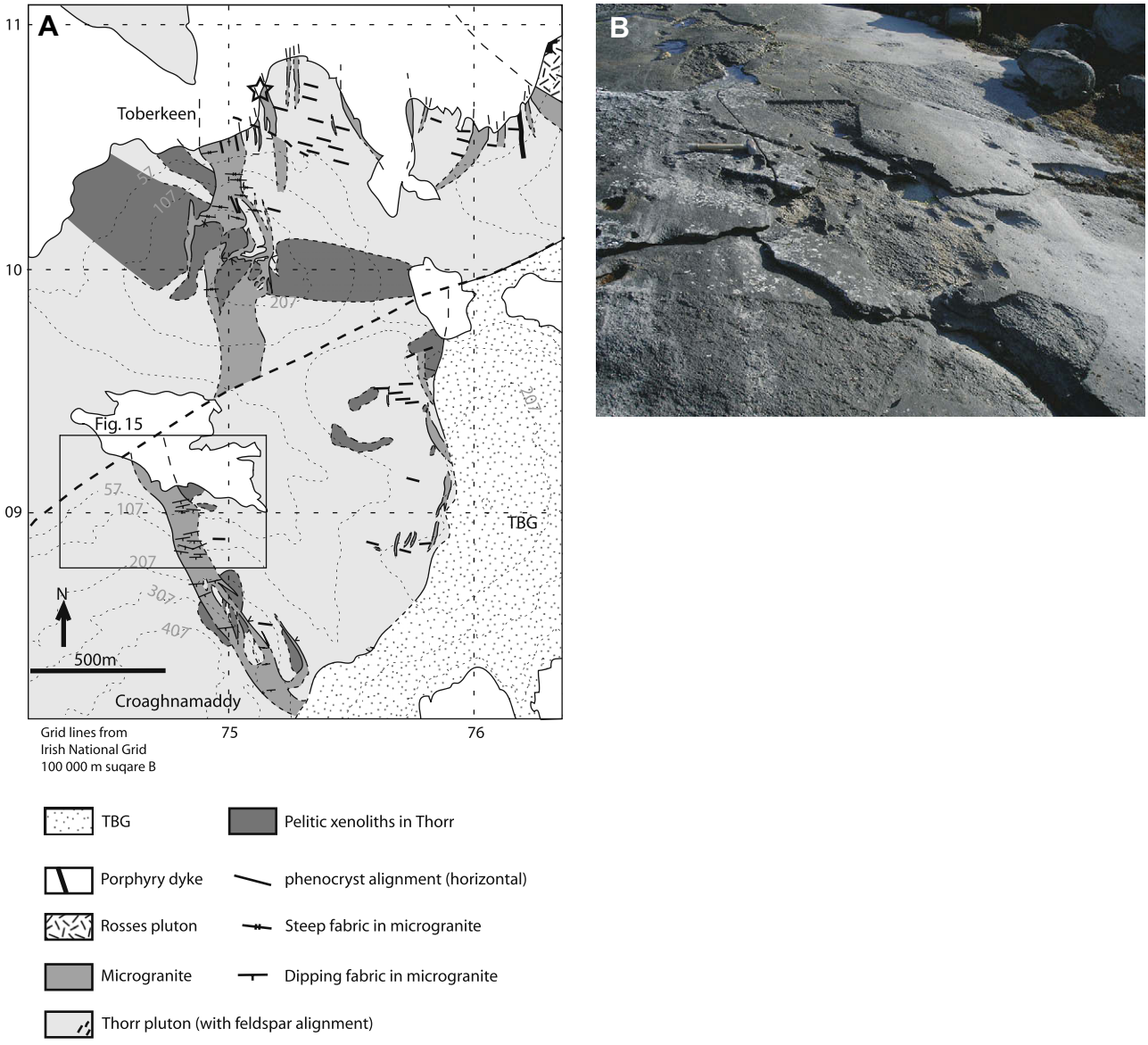

Fig. 8. (A) Map of the area just west of Toberkeen (see Fig. 2, contours are in feet). (B) Field photograph of an outcrop of a microgranite sheet (location indicated in part A with a star) taken in the early evening when the low angle of the sun reveals the relief of smooth microgranite and rough (coarse grained) tonalite. Numerous xenoliths of tonalite are seen with a variety of angular to lobate shapes.

Fabrics in these sheets are weak and subhorizontal, although an east-west alignment of plagioclase is often observed. The weak magmatic-state fabric is reflected in a preferred orientation of xenoliths and rare mafic enclaves of a finer grained microgranodiorite, the latter mainly in the Crovehy sheet, which in 3D are flattened in a roughly subhorizontal plane with an east-west trending long axis (Fig. 7B). In these large sheets, subtle internal contacts are noticed indicating that these sheets are multiple (Fig. 7C).

At the southern margin of the largest sheet (Crovehy , location 54°65'59"N, 8°16'41"W) a glacial pavement exposes a xenolith–

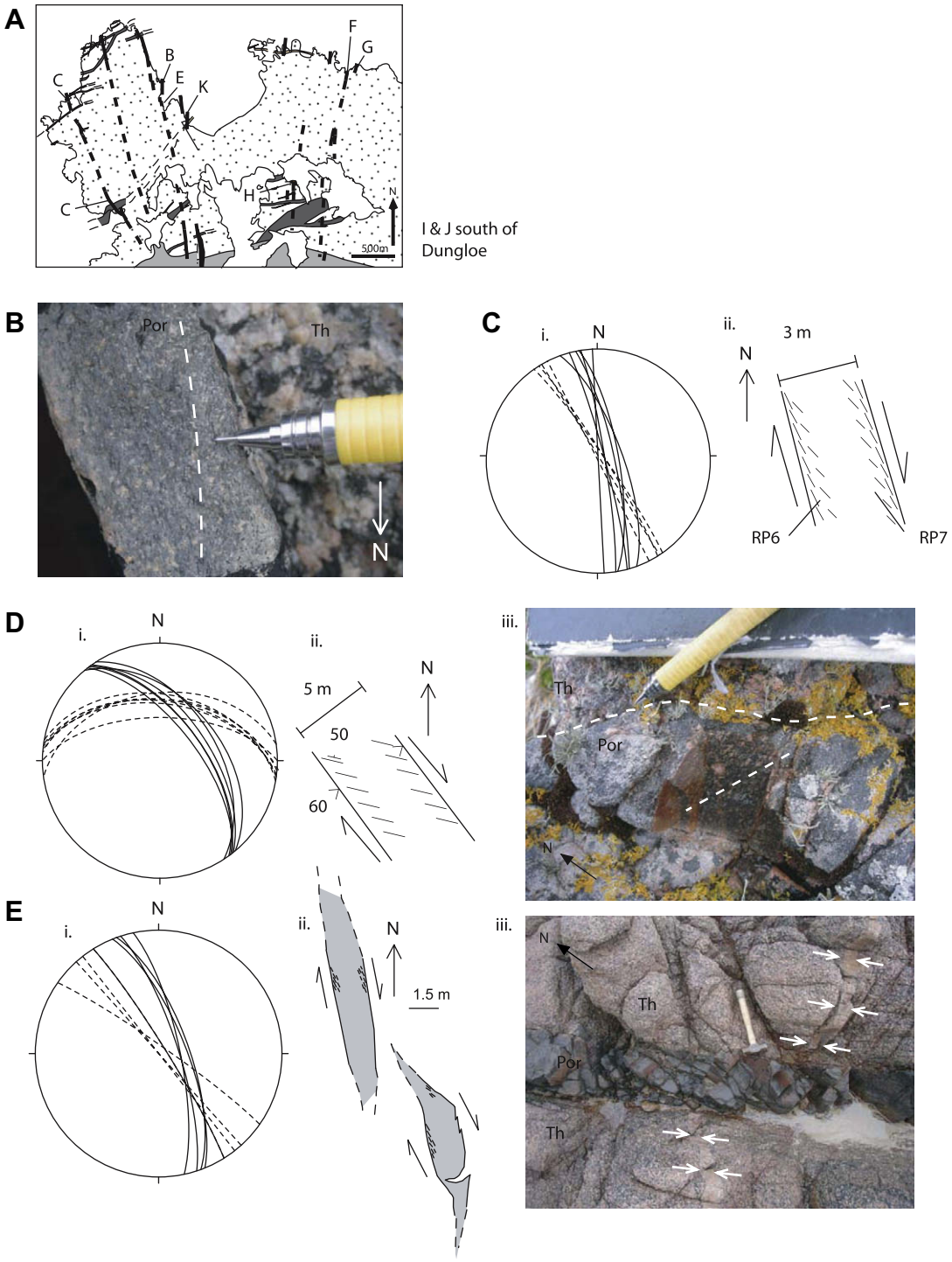

Fig. 9. Visible fabric data from the porphyry dykes. (A) Sketch map showing the locations of where fabrics were measured in parts B–H. (B) Field photograph of the margin of a porphyry dyke. A fabric defined mainly by biotite (highlighted with a dashed white line) is observed at an apparent low angle to the margin between the porphyry (Por) and Thorr granodiorite (Th). (C) i. Stereographic projection of contacts (solid lines) and visible fabrics (dashed lines) measured at this locality; and ii. sketch map of the fabric–contact relationships indicating a dextral sense of shear. (D and E) i. Stereographic projection of contacts (solid lines) and visible fabrics (dashed lines) measured at this locality; ii. sketch map of the fabric–contact relationships indicating a dextral sense of shear; and iii. field photograph displaying these fabric–contact relationships. (F–I) i. Stereographic projection of contacts (solid lines) and visible fabrics (dashed lines) measured at this locality; and ii. sketch map of the fabric–contact relationships indicating a dextral sense of shear. (J) Stereographic projection of contacts (solid lines) and visible fabrics (dashed lines) measured at this locality. (K) Field photograph showing xenoliths of Thorr granodiorite displaying lobate contacts. This is the only locality in which these have been found.

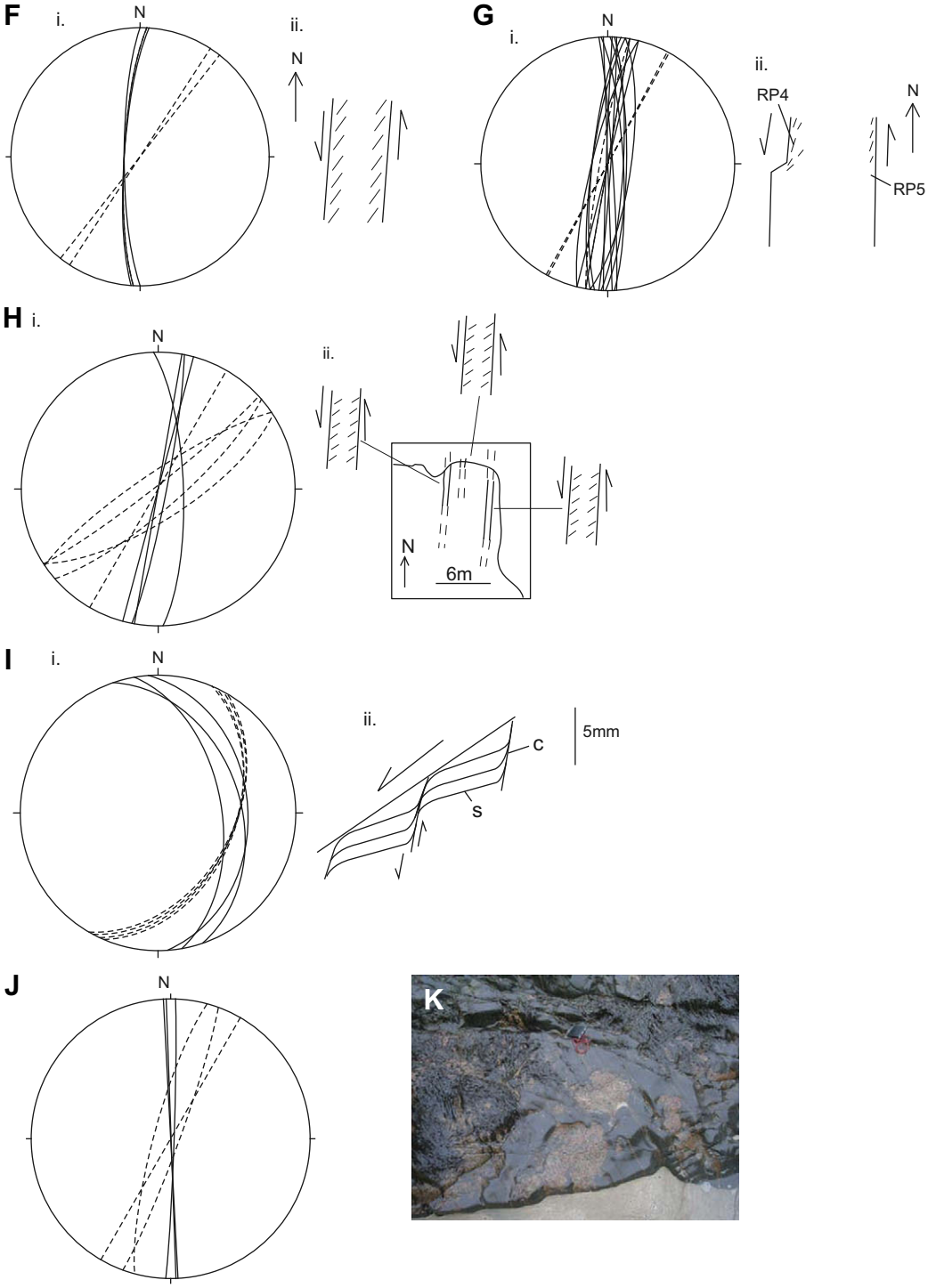

Fig. 9. (*continued*).

strewn base with gently dipping fabrics (see Supplementary map). Xenoliths are of Thorr granodiorite and a quartz rich granitoid of unknown affinity. Xenoliths are aligned with their long axes parallel with strike of the microgranite sheet. The margin of the sheet cuts a mineral alignment in the Thorr at a high angle. Xenoliths of Thorr also display an internal fabric but this fabric is rotated and is aligned east-west parallel with the strike of the sheet and alignment of xenoliths. Pitcher (1953a) suggested the quartz rich granite xenoliths were related to a nearby stock, which crops out ~100 m perpendicular to strike. However, this cannot be confirmed here as the east-west alignment and rotation of fabric of the xenoliths suggests that they have been transported along strike in the microgranite. These quartz rich granitoid xenoliths could be related to any other monzogranite of this Batholith.

In a few southerly locations of the Crovehy sheet, a steeply dipping east-west trending fabric is observed. This fabric is late as it deforms all members of the microgranites and late pegmatite dykes and is concomitant with deformation associated with the Main Donegal shear zone (Hutton, 1982; Stevenson et al., 2008).

In the southwest (between Dungloe and Toberkeen) there are several small microgranite sheets and one main sheet, which strikes roughly north–south and dips moderately west (Figs. 2 and 8).

In this main sheet, a steeply dipping east-west trending fabric is more obvious and is parallel with deformation associated with a splay of the Main Donegal Granite shear zone (Stevenson et al., 2008). In lower strain portions of this sheet a weak north–south fabric is preserved. Here, as in the northwest, xenoliths of Thorr tonalite exhibit a range of contact relationships from sharp angular to lobate to gradational (Fig. 6A and B).

2.4. Porphyry dykes

Visible fabrics are often oblique to the margins within a few centimetres of the margins (Fig. 9). These fabrics are defined by biotite and plastically deformed feldspars and are therefore solid-state (e.g. Fig. 9B and Diii). The obliquity is usually consistent on each margin of the same dyke indicating shearing by movement of the dyke walls (Berger, 1971). The sense of shear from sheared fabrics and offsets determined in dykes that trend NNW is dextral (e.g. Fig. 9B–E) and from those trending NNE it is sinistral (Fig. 9F–I). Not all dykes that exhibit offsets of earlier features exhibit solid-state fabrics (e.g. Fig. 9Eiii) suggesting that the dykes were emplaced during the cessation or waning of a period of tectonic strain.

3. Anisotropy of magnetic susceptibility

Anisotropy of magnetic susceptibility (AMS) can reveal the preferred orientation of paramagnetic minerals and the preferred orientation and/or distribution of ferromagnetic minerals (principally biotite and magnetite respectively). Thus, the orientation of the principal axes of the susceptibility ellipsoid can be used as a proxy for the orientation of mineral alignment fabrics and can be a powerful tool for constraining or defining very subtle fabrics in 3D (Tarling and Hrouda, 1993; Bouchez, 1997). However, because of the potential conflicting contribution from different magnetic grains, direct strain analysis is very difficult and detailed petrological observation and complimentary magnetic techniques (e.g. thermomagnetic analysis) of the contributing mineralogy and the formation of any fabric is required before any conclusions can be drawn concerning magma flow directions (e.g. Stevenson et al., 2007a; O'Driscoll et al., 2008).

The magnetic susceptibility tensor may be pictured as an ellipsoid with six independent quantities, which includes three principal susceptibility magnitudes, $K_1 \geq K_2 \geq K_3$, and a corresponding

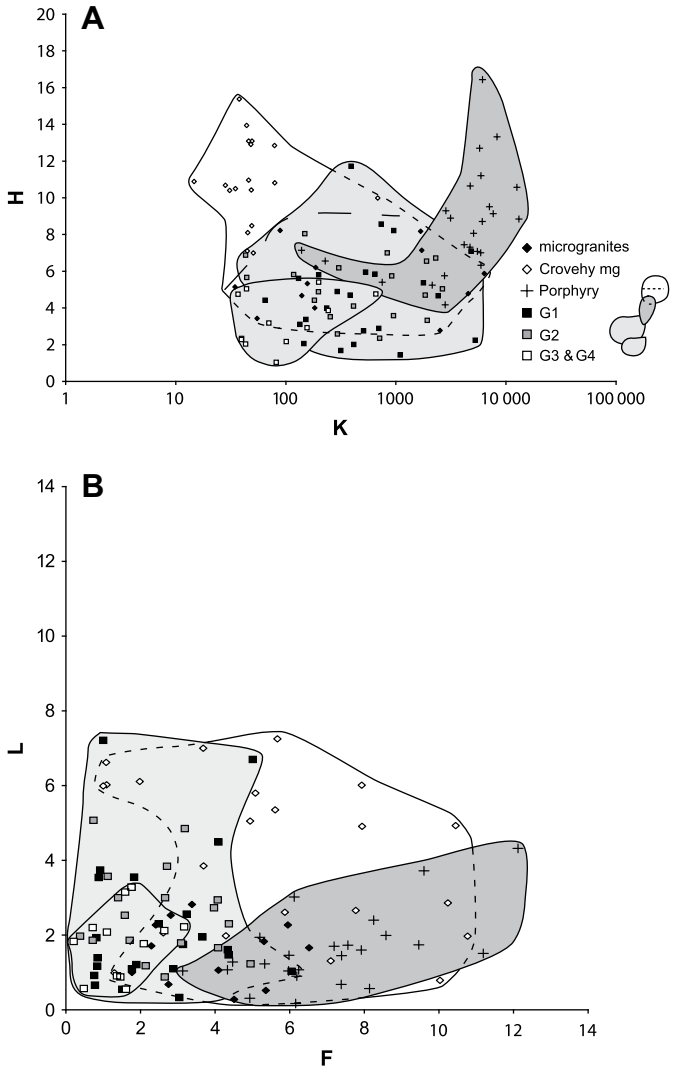

Fig. 10. (A) *H* plotted against *K* for all samples from the Rosses Complex. Data for each unit has been outlined and background shaded in varying white to grey for clarity. (B) *L*/*F* plot for all samples from the Rosses Complex, symbols and outlines are as in part A.

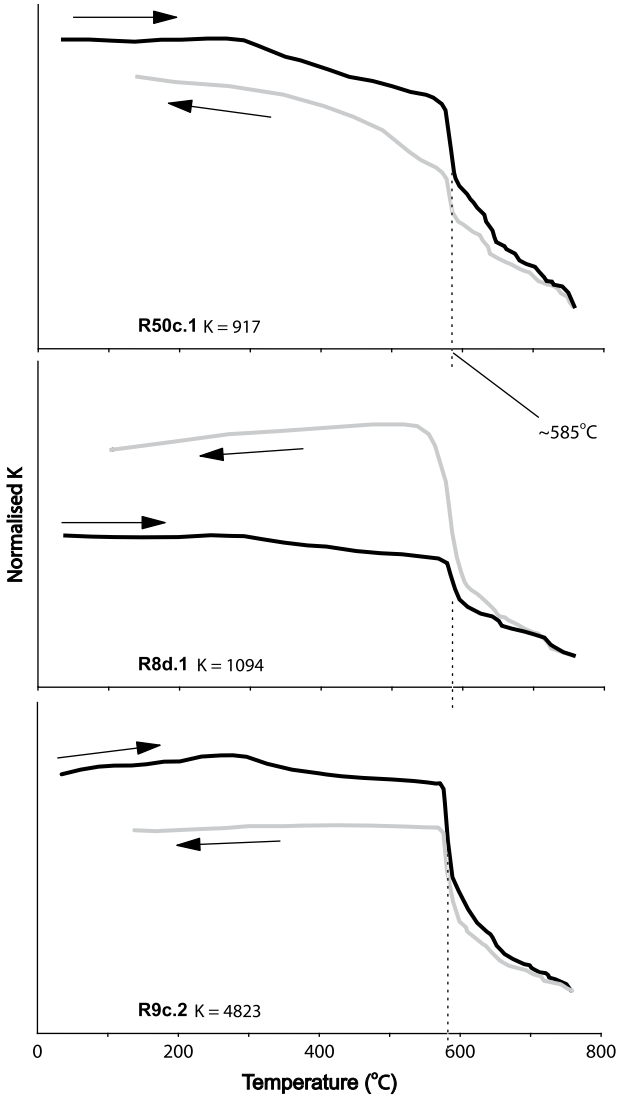

Fig. 11. Susceptibility with varying temperature for three representative samples from the Rosses Complex. On each plot, the heating curve is in black and the cooling curve in grey. The susceptibility (*K*) is shown for each sample. Heating curves indicate the Curie temperature of magnetite (~585 °C).

set of three orthogonal principal axis directions. It is conventional to recast the three magnitude parameters in terms of three parameters, which together reflect the "size", "shape" and "strength" (or ellipticity) of the ellipsoid. The three parameters adopted here (cf. Owens, 1974) are:

$$K_{mean} = (K_1 + K_2 + K_3)/3$$

$$L = (K_1 - K_2)/K_{mean}$$

$$F = (K_2 - K_3)/K_{mean}$$

where K_{mean} is effectively the size, a plot of the magnetic lineation L against the magnetic foliation F indicates graphically the shape of the ellipsoid where prolate ellipsoids lie near the L axis, oblate ellipsoids near the F axis, triaxial ellipsoids occupy middle of the plot. Although the three quantities K_{mean}, L and F are sufficient to define the magnitude parameters of the ellipsoid, it is convenient to define another parameter, $H = L + F = (K_1 - K_3)/K_{mean}$ to indicate the strength of the magnetic fabric.

In order to assess the AMS of the Rosses Complex a suite of 113 oriented block samples in total were collected; 54 from the pluton, 35 from the microgranite sheets and 24 from the porphyry dykes. 6–12 sub-specimens were drilled from each sample in the lab by the method outlined by Owens (1994) and measured on an AGICO KLY3-S Kappabridge (an induction bridge operating at a field of 377 μT and a frequency of 875 Hz) at the University of Birmingham. Results are reported for block averages of specimen AMS tensors, normalised by specimen mean susceptibility, on the assumption that the specimens from a block are representative of a homogeneous multinormal population (Figs. 10–17). The tensor-averaging process (Jelínek, 1978; Owens, 2000) allows for the characterisation of within-block variability through, for example, the calculation of 95% confidence limits on directions and magnitude parameters. The variation of susceptibility with temperature was measured using an AGICO CS-3 oven attachment to the Kappabridge on powder samples of ~2 g.

3.1. AMS results

The AMS results for all members of the Rosses Complex are displayed in Fig. 10 (and Supplementary table).

3.1.1. Microgranite sheets

Susceptibility (K_{mean}) values for the microgranite sheets are 8–6339 × 10^{-6} (in the SI system) with H values ranging between 2 and 15%. The shape of anisotropy is generally in the triaxial–oblate field except for a few samples from the Crovehy sheet in which L is much greater than F.

3.1.2. Rosses Pluton

Susceptibility values for G1 and G2 are 37–5257 × 10^{-6} (in the SI system) with H values ranging between 1 and 12%. In G3 and G4 K_{mean} values are 37–658 × 10^{-6} with H values ranging between 1 and 5%.

3.1.3. Porphyry dykes

K_{mean} values for the porphyry dykes are 139–13124 × 10^{-6} with H values ranging between 4 and 16%. The shape of anisotropy is generally in the oblate field.

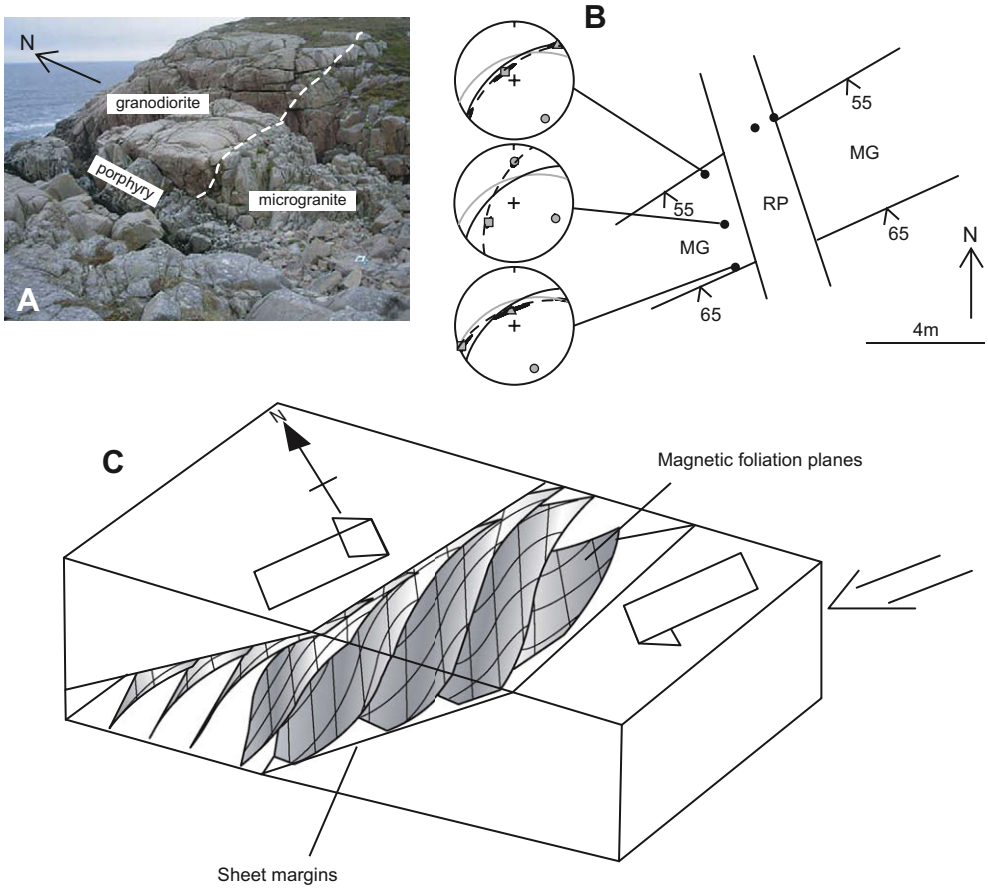

Fig. 12. (A) Field photograph showing the relationship between Thorr granodiorite, a microgranite sheet and a porphyry dyke. (B) Sketch map of the locality, dip of microgranite (mg) contacts is shown. AMS sample points are indicated and orientation data from these samples plotted stereographically; K_1 axis – square, K_2 axis – triangle and K_3 – circle. Also plotted on the stereonets are great circles for the contacts: upper contact – solid black line, lower contact – solid grey line, and magnetic foliation – broken line. (C) 3D visualisation of the fabric geometry in the microgranite sheet displaying how the AMS foliation is subparallel to the contacts but strikes anticlockwise in the centre.

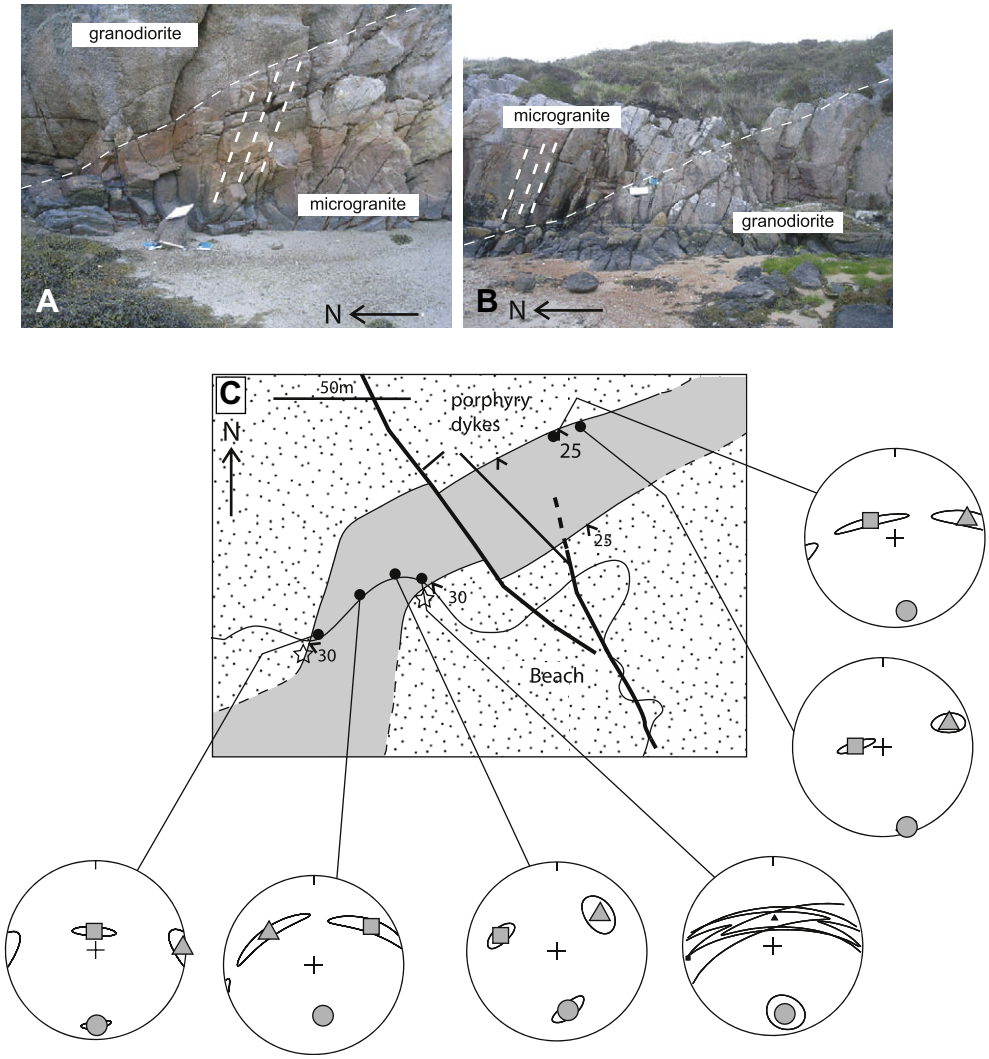

Fig. 13. (A) Field photograph showing the upper contact of a microgranite sheet. (B) Field photograph showing the lower contact of the same sheet with the apparent dip of visible fabric (feldspar alignment) indicated. (C) Sketch map of this locality (microgranite is grey). The dip of contacts is also shown. Indicated are AMS sample points and the orientation data from these samples plotted stereographically (axis labelled as in Fig. 12). Note the dextral offset of microgranite across an NE striking porphyry dyke.

3.2. Magnetic minerals

The mineralogy of each member of the Rosses Complex is broadly similar (Pitcher, 1953b; Mercy, 1962; Hall, 1966). Accessory minerals in all members include oxides, identified from reflected light microscopy as magnetite or titanomagnetite with small amounts of haematite.

Biotite has been identified as a fabric-forming phase in this study and by Pitcher (1953b). However, thermomagnetic analyses reveal a step in the thermomagnetic (temperature vs. susceptibility) consistent with the curie temperature of magnetite confirming magnetite is as a significant magnetic carrier (Fig. 11). Microscopic observations reveal that magnetite is usually associated with biotite either growing close to the margins of biotite grains or along cleavage planes. Stevenson et al. (2007a) established a mimetic relationship between biotite and magnetite for the Trawenagh Bay Granite, where high-field susceptibility measurements confirmed parallelism between paramagnetic and ferromagnetic anisotropies, and heating experiments showed that secondary magnetite grew along biotite cleavage planes. Thus the AMS fabric orientation could be interpreted as essentially controlled by the orientation of biotite across the range of susceptibility values. Given the similarities in mineralogy between the Trawenagh Bay Granite and the Rosses Complex, the same fabric model is extended to this study.

4. AMS fabrics in the Rosses Complex

4.1. The microgranite sheets

Two main sheets were sampled in the northwest. The AMS fabrics in these sheets support the observation that visible fabrics do not parallel the margins of the sheets. In sheet 1, north of Kincasslough (Fig. 12), the magnetic foliations are parallel to the margins but strike ~30° anticlockwise in the centre of the sheet (Fig. 12B). These AMS fabrics indicate a reverse-oblique-dextral sense of shear (Fig. 12C). In sheet 2, just west of Kincasslough (Fig. 13), AMS foliations are not consistently parallel to the sheet contacts, but are parallel to the nearest contacts of the Rosses Pluton (Fig. 12C). AMS lineations in these sheets are orientated broadly down dip or oblique to dip.

In the larger eastern sheets, AMS foliations are usually gently dipping or roughly subhorizontal, AMS lineations trend roughly east-west. Exceptions are in the southern most portions of the Crovehy sheet where the AMS foliations dip steeply and strike east-west (Fig. 14).

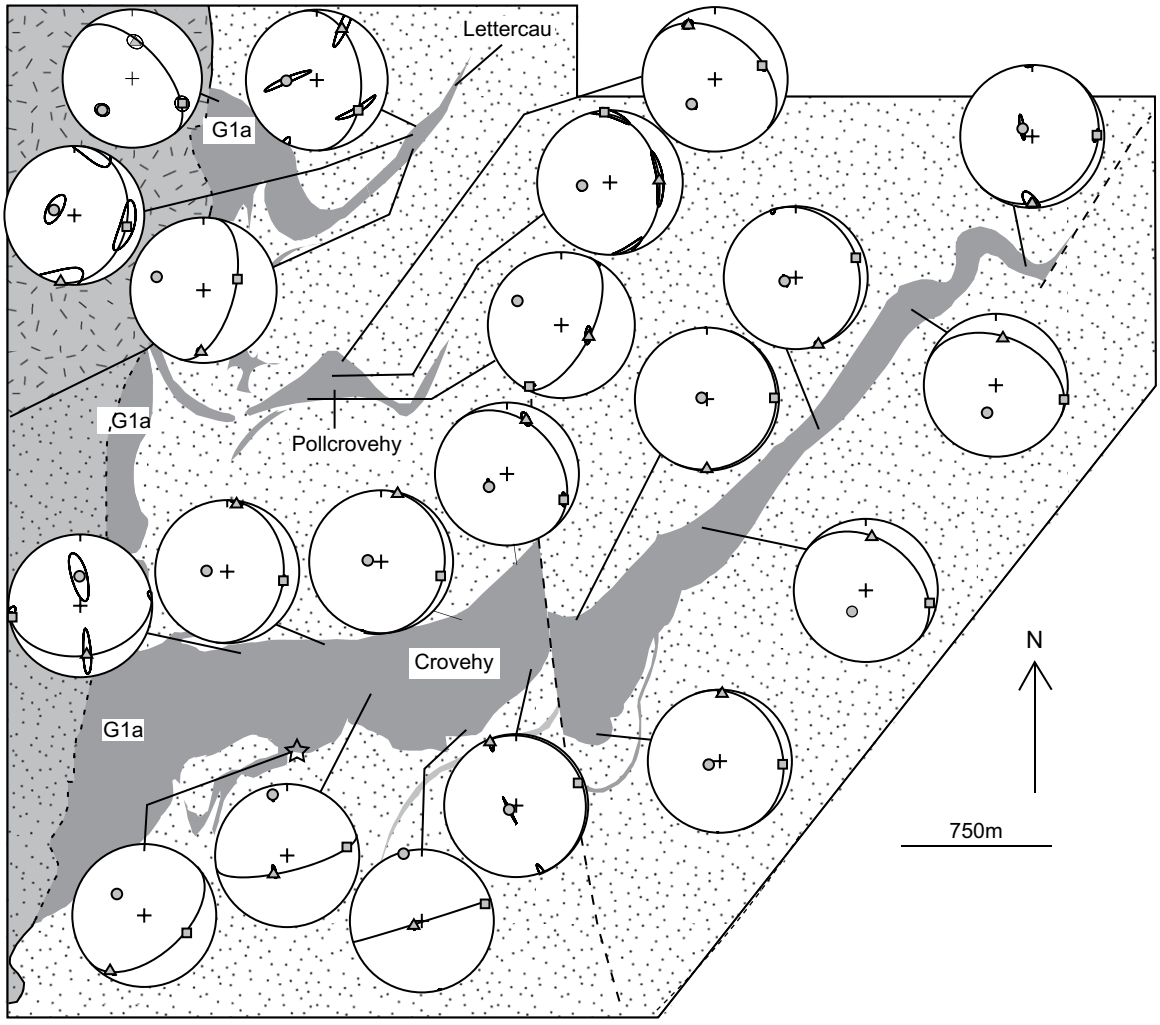

Fig. 14. Sketch map of the microgranite sheets in the east. Lithology fills are as in Fig. 1. AMS data is plotted stereographically; symbols are as in Fig. 12. Note the generally subhorizontal dip of the magnetic foliation and the east-west gently plunging lineation Star indicates the location of the Supplementary map.

In the southwest three samples were collected from the main sheet. In the two most southerly samples, fabrics dip steeply and strike east-west, consistent with the late cross cutting shear zone fabric. In the third sample, the fabric dips parallel with the contact of the sheet consistent with the early fabric (Fig. 15).

4.2. The Rosses Pluton

In G1 and G2, magnetic foliations are usually parallel with the outer contacts, consistent with the microscopic fabrics measured by Pitcher (1953b), essentially defining a dome shaped pattern. Magnetic lineations are disposed roughly east-west about the dome shaped foliation pattern (Fig. 16). However, in G3 and G4 magnetic fabrics are not well preserved.

4.3. Porphyry dykes

Magnetic foliations usually parallel the visible fabrics supporting the obliquity to dyke margins (e.g. Fig. 17C,H and J). Those with no visible fabrics often show magnetic foliations that support the sense of shear of similarly orientated dykes, i.e. those oriented NNW are dextral, and those NNE are sinistral. Magnetic lineations are much less consistently orientated, although this is unsurprising considering the dominantly oblate magnetic fabric. Subsequently, little can be drawn concerning magma flow or direction of emplacement of these dykes.

5. Discussion: magma flow and deformation

The earliest components of the complex, the microgranite sheets in the east, contain gently dipping magmatic-state foliations (visible and magnetic) and east-west, gently plunging magnetic lineations. These sheets seem to preserve an early stage of magma emplacement where the sheets dip gently to moderately northward.

The microgranite sheets in the northwest contain magnetic fabrics that are consistently parallel to the margins of the main Rosses Pluton rather than the microgranite sheets. These fabrics must have been imposed upon these sheets (post-emplacement) by forceful emplacement of the main Rosses Pluton. The dip of the sheets varies between $\sim 20^\circ$ and $\sim 70^\circ$ to the northwest. It may be that these sheets represent an interconnected plexus of bridges and partial bridges (e.g. Nicholson and Pollard, 1985). The variable dip reflects tilting during the emplacement of the Rosses Pluton so that they all now all dip northwest. The uniform strike of these sheets suggests that their axes of disposition, deformation or tilting, possessed an apparently east-west trend indicating an east-west propagation direction for these sheets.

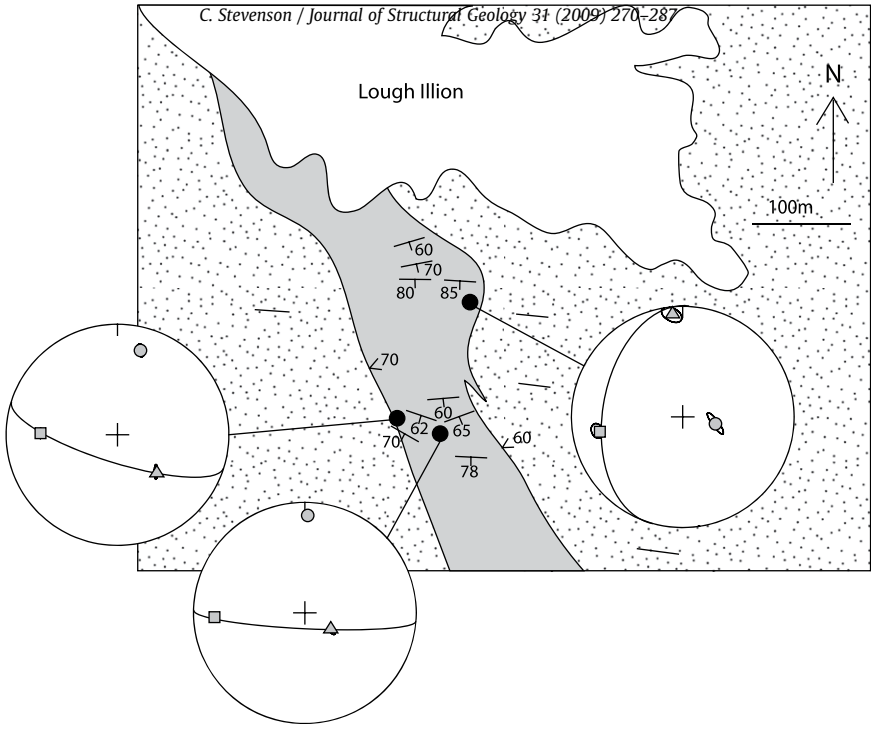

Fig. 15. Sketch map of a microgranite sheet (grey) in the southwest, with visible fabric orientations marked with strike and dip bars and stereographic plots of AMS orientation data. Observed fabric trace in the Thorr granodiorite is marked with a dash. Note the steep magnetic foliations roughly parallel to visible fabrics, presumably tectonic related, and gently dipping fabric from one AMS station parallel to the margin, possibly primary magmatic.

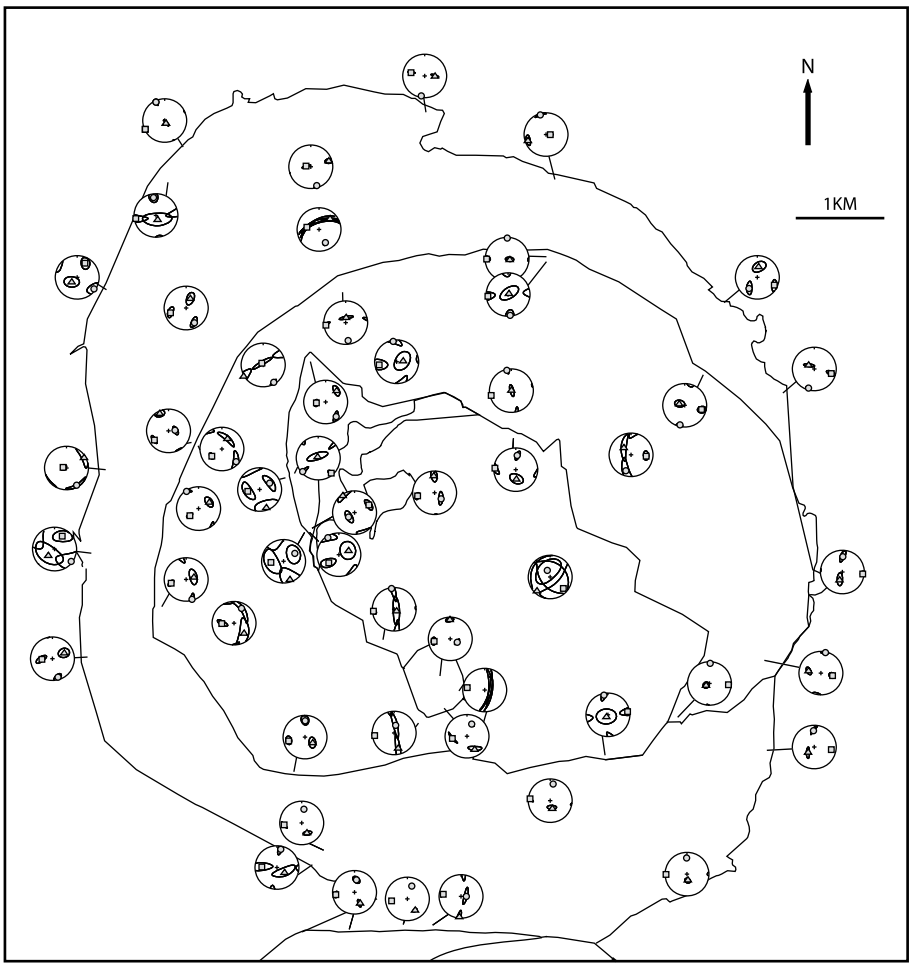

Fig. 16. Stereographic plot of AMS orientation data for the main Rosses Pluton. The margins of the internal units of the pluton are shown in outline and all other lithologies omitted for clarity. Symbols are as in Fig. 12.

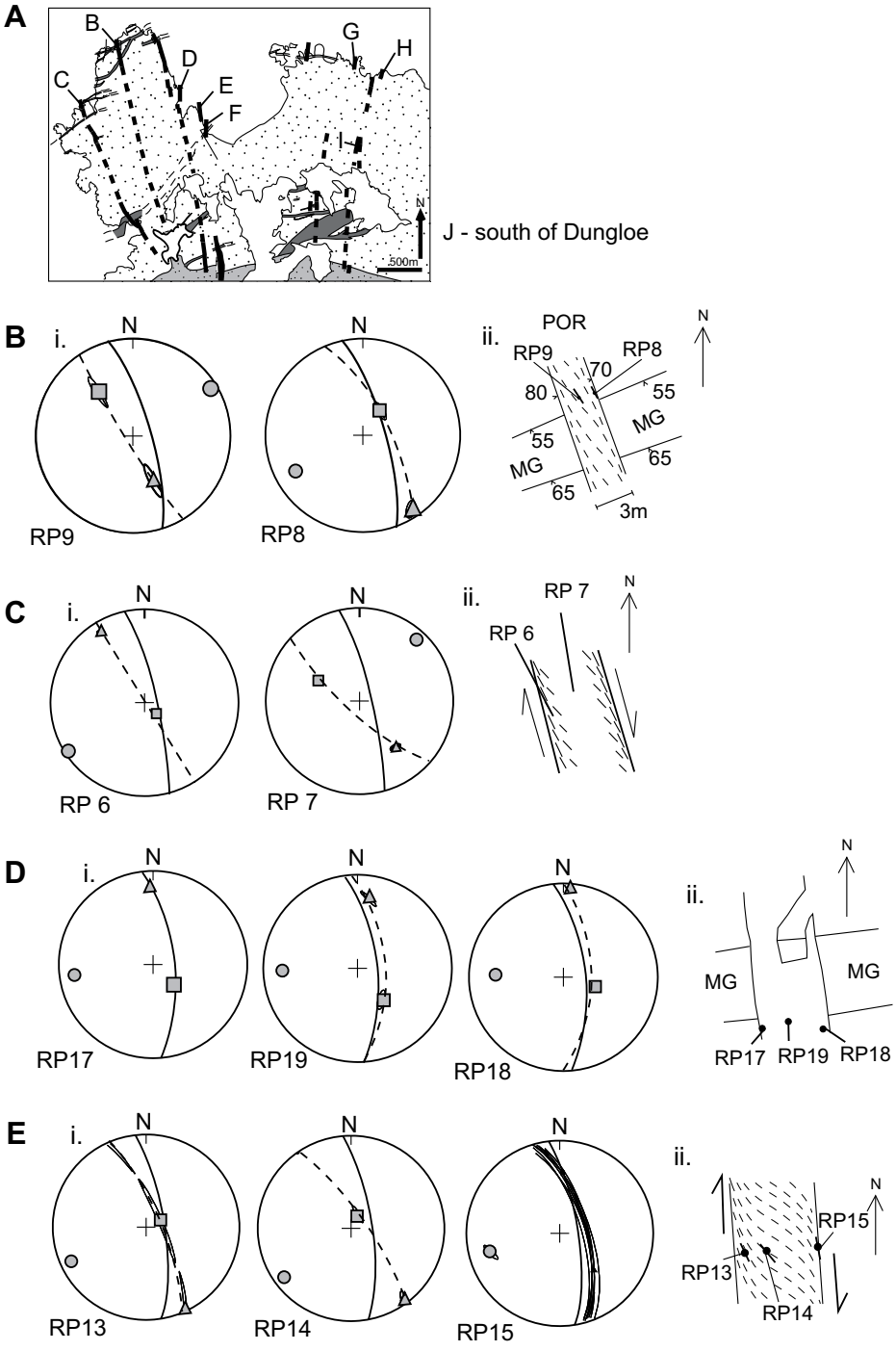

Fig. 17. AMS data for the porphyry dykes. (A) Sketch map showing the location of sample stations. (B–J) i. stereographic plot of AMS orientation data, symbols as in Fig. 12 plus solid great circles – dyke margin, dashed great circles – AMS foliation; and ii. sketch showing the interpretation of sense of shear.

The sheets in the northwest and southwest seem to be affected by post-emplacement events. These include deformation from the emplacement of the Rosses Pluton or deformation associated with the Main Donegal Granite shear zone respectively.

In the main Rosses Pluton, the magnetic fabrics do not support vertical magma flow. Instead, the east-west disposition of the lineations tends to suggest lateral inflow. Furthermore, the apparent tilting of the earlier microgranite sheets and the deflection of Thorr fabrics indicate a forceful mechanism involving lateral emplacement and vertical thickening of the pluton. This proposed model is similar to the Iron Axis Pluton, USA (Petronis et al., 2004) and the Eastern Mourne Pluton, N. Ireland (Stevenson et al., 2007b). The tilting of microgranites in the west and shearing of microgranite in the northwest (Figs. 12 and 13) is consistent with magma emplaced from east to west. The small bodies of coarse quartz rich granite occurring to the east may be small cupolas of an eastward subterranean extension of G2. The apparently cross cutting fabrics on the western margin of G1, however, require explanation. This is similar to the Trawenagh Bay Granite's western margin. Stevenson et al. (2008) suggested that the Trawenagh Bay Granite abutted against a steeply dipping passive westward margin, controlled by the regional east-west tectonic extension, which came into effect in

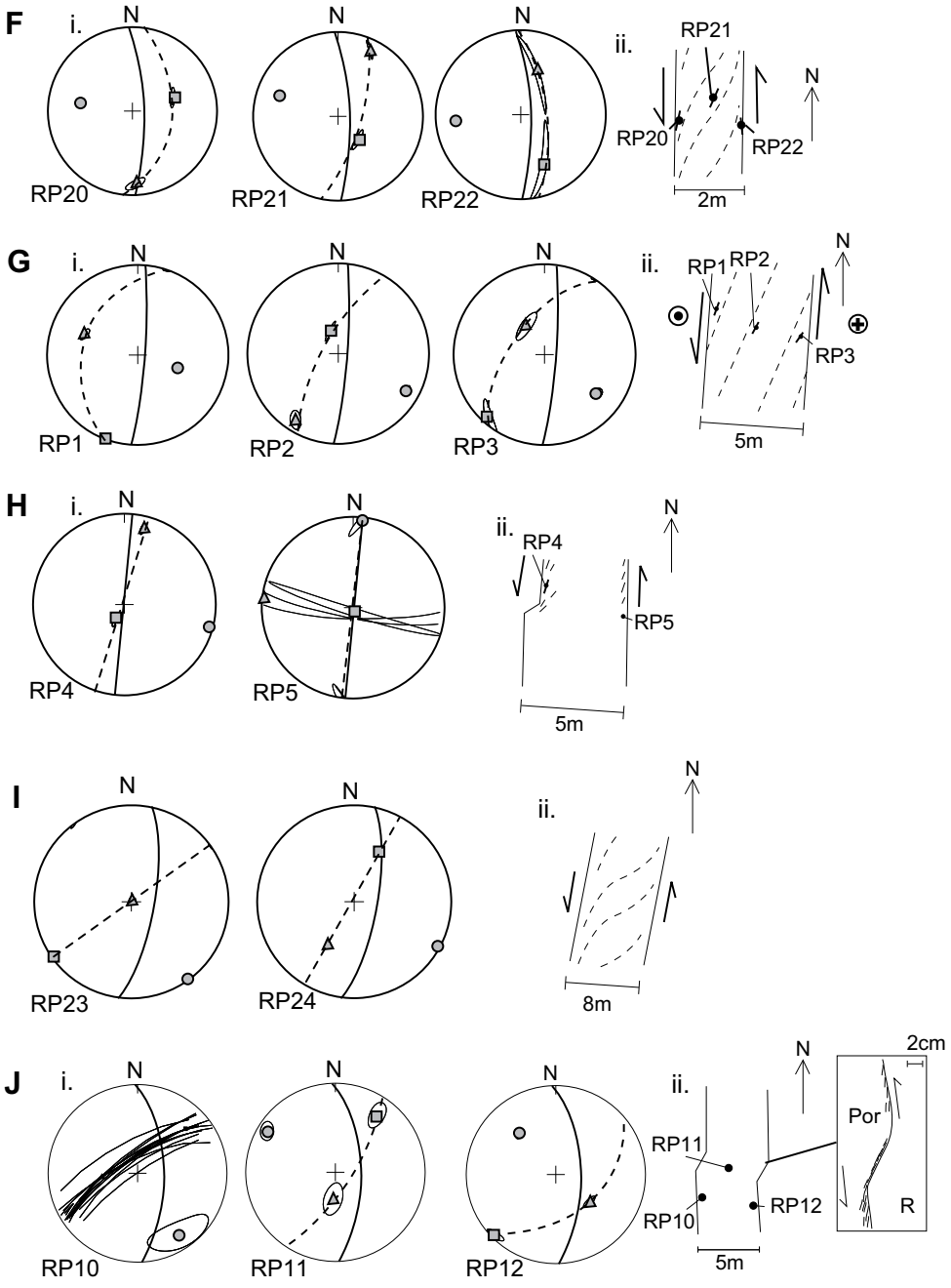

Fig. 17. (*continued*).

the distal portion of the pluton that was fed from the east. It is suggested here that this may also account for the cross cutting nature of this portion of the Rosses G1 margin.

The G3 and G4 units cannot easily be explained from this data. This is a similar situation to the G3 unit of the Trawenagh Bay Granite, which Stevenson et al. (2007a) thought to be a cupola related to another sheet. This may be the case for the G3 and G4 units of the Rosses Pluton, where the fracture control envisaged by Pitcher (1953b) may apply at least to the more evolved and pegmatite rich G3 unit. However, the sheet from which G3 emanated would be similar in composition and texture to the G1 and G2 units.

Thus, the Rosses Complex was emplaced laterally from east to west. The major implication of this is that, like the Trawenagh Bay Granite (Stevenson et al., 2007a, 2008), it was derived from magma within the Main Donegal Granite. It is an example of lateral emplacement of magma where the ascent was controlled by a major crustal shear zone – Main Donegal Granite – and was not directly subjacent.

The element of fracture control in the emplacement of this complex has also been put into context. The initial and main stages of emplacement involved the propagation and subsequent vertical thickening of subhorizontal sheets. Only the final stages of emplacement (units G3 and G4 of the Rosses Pluton) may have occurred due to passive subsidence into a subjacent sheet.

This second phase of passive emplacement may have been preceded by the intrusion of the porphyry dykes, which record in their visible and magnetic fabrics an east-west oriented extension. The transition from forceful to passive emplacement is possibly due to a waning magma supply within a longer lived tensional strain field. In the early stages, magma supply was such that magma

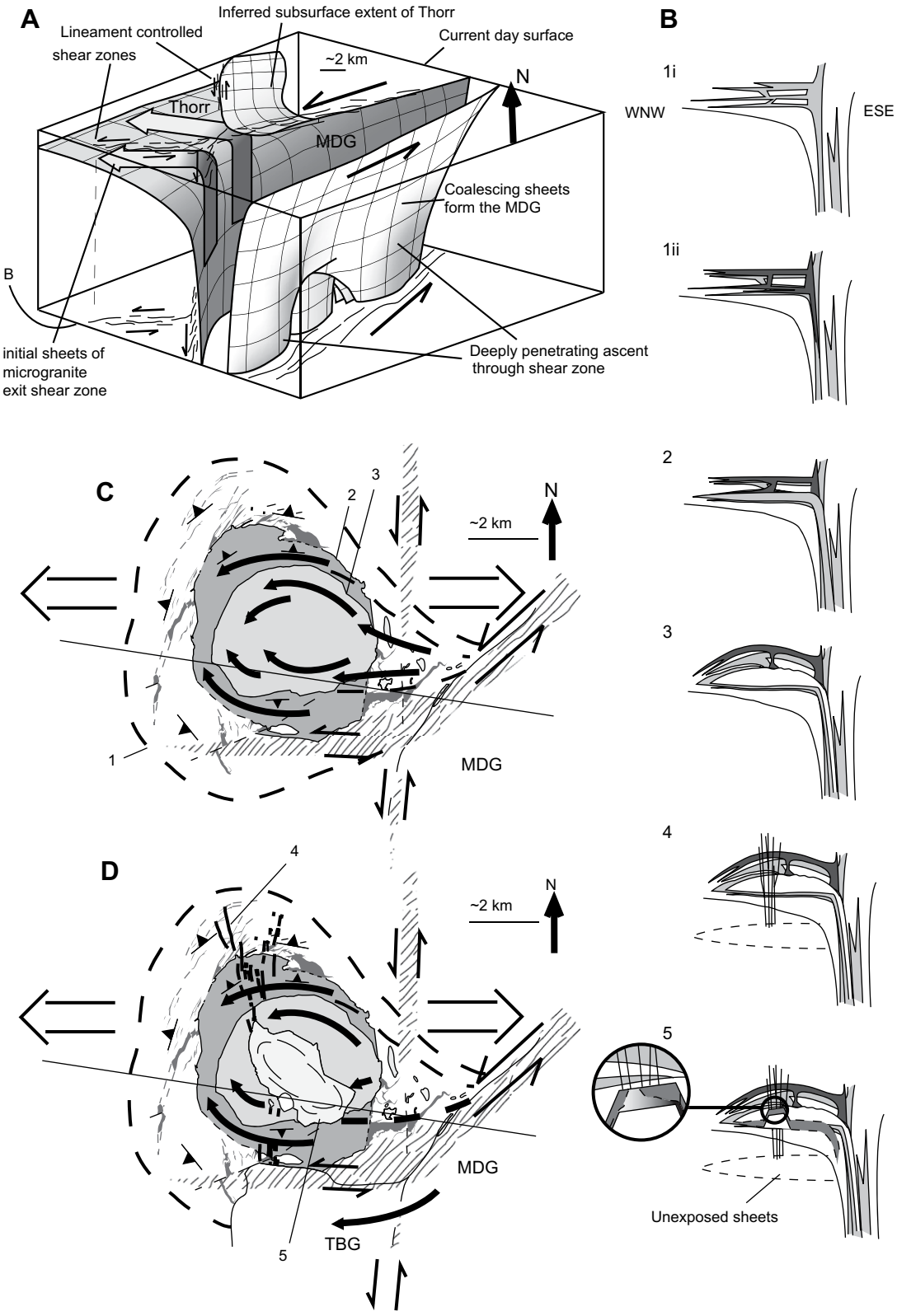

Fig. 18. Final model. (A) 3D box diagram showing a portion of the floor of the Thorr Plutons and a large part of the Main Donegal Granite (MDG) at the time of the initial microgranite sheet emplacement extending vertically from the present day surface to ~6–8 km. (B) Sketch cross section roughly corresponding to the SE side of the box of part A (and to roughly the same scale), showing the emplacement of each member of the Rosses Complex. 1 i and ii – microgranite sheets, 2 – G1, 3 – G2, 4 – porphyry dykes, 5 – G3 (inset shows G4). (C) Summary of map based on present day exposure level of the main forceful phase (parts B1–B3). Note that the Trawenagh Bay Granite to the south has not yet been emplaced. Large open arrows show the regional east-west tensional tectonic strain. Smaller shear couple arrows show the main shear zones (after Stevenson et al., in press). Thick dashed line represents the postulated (unexposed today) extent of the microgranite sheets and G2. Strike bars with a dip barb demonstrate how the microgranite sheets and fabrics in G1 dip away from the forceful and substantive G2 dome. Thick arrows represent the interpreted magma flow pathways from AMS data. The line of section for part B is shown. (D) Summary of map based on present day exposure level of the main passive phase (parts B4– B5). Note that the Trawenagh Bay Granite to the south has now been emplaced sometime just after the porphyry dykes (B4). All other arrows and symbols are as on part C.

pressure could overcome east-west tectonic extension and effect horizontal fractures. As magma supply waned (or was switched to another site) so too did magma pressure and vertical north–south trending dykes were emplaced from subjacent sheets.

It is also noteworthy that the timing of emplacement of the Thorr Pluton and Rosses Pluton does not seem to involve such a large gap as has previously been accepted. The deflection of Thorr fabrics without any obvious solid-state strain plus the evidence for liquid–liquid relations between Thorr granodiorite and some of the microgranite sheets suggests that there was actually a very short, if not overlapping, time gap. This is significant given that the Thorr Pluton is regarded as the oldest member of the batholith whereas the Rosses Complex is among the youngest (Pitcher and Berger, 1972; Halliday et al., 1980; O'Connor et al., 1982).

Finally, the evidence presented here for lateral emplacement from outcrop data and fabric interpretation (both visible and from AMS measurements), is at variance with the significant negative gravity anomaly centred over the Rosses Pluton (Young, 1974). This suggests a significant amount of low-density material (likely monzo–leucogranite) beneath the Rosses, however, this need not be the ascent route for Rosses magma. Instead, it could indicate a series of similar plutons to the Rosses in a Christmas tree laccolith style stack (cf. Corry, 1988; Rocchi et al., 2002). Each of these may have been emplaced laterally in a similar fashion to the Rosses, from the Main Donegal Granite, their positioning controlled by some underlying lower crustal structure (Stevenson et al., 2008) (Fig. 18).

It is worth noting that the latest stage is the dominant mineralising stage and is concomitant with passive fracture controlled emplacement allowing fluids to circulate. This fracture related style of emplacement is crucial in the formation of significant epithermal and porphyry ore deposits as it allows fluids to circulate as well as providing space for magma (e.g. Titley and Heidrick, 1978; Titley et al., 1986; Williams et al., 1999; Garza et al., 2001; Chernicoff et al., 2002; Guillou-Frottier and Burov, 2003; Engvik et al., 2005; Garza-Gonzalez et al., 2006). Fluid inclusion studies by Conliffe and Feely (2006) identified a late magmatic fluid stage associated with beryl mineralisation in the Rosses G3 and G4 greisen. They suggest that this fluid evolved by a pressure drop during cauldron subsidence. If the entire complex was emplaced in this way, given the relatively evolved nature of all the magmas involved, this mineralisation (together with associated pegmatite, aplite and greisens) should be associated with all members of the complex. The model presented here helps to explain the timing and driving mechanism of the pressure drop within the overall emplacement model and will have application in predicting mineralisation associated with this style of granite emplacement.

6. Conclusions

The Rosses Complex was emplaced in four main stages (Fig. 18): the first two were lateral and forceful from east to west and then the third and fourth phases were dominantly passive and brittle, phase 4 at least arising from unexposed sheets emplaced during phases 1 and 2.

Phase 1: A plexus of subhorizontal sheets of microgranite was intruded east to west. These sheets appear to become generally thinner and more numerous proceeding east to west (Fig. 18A,B1i and B1ii).

Phase 2: The emplacement of G1 and G2 of the Rosses Pluton, which also occurred in an east to west direction. This pluton was fed laterally by a largely unexposed conduit. Only small cupolas of G2 magma rising from this feeder conduit are exposed to the east of the pluton. The emplacement of the Rosses Pluton was forceful as it deflects fabrics in the surrounding Thorr Pluton and tilts and deforms microgranite sheets in the northwest and west (Fig. 18B2 and C).

Phase 3: This phase began with the intrusion of the porphyry dyke swarm, which record east-west extension. It is not clear where these sheets originate from but they may have a similar origin to phase four in unexposed subjacent sheets (Fig. 18B3).

Phase 4: This dyke swarm is then followed by the emplacement of the G3 and G4 units of the Rosses Pluton, which are probably cupolas of a further sheet of the second phase. These cupolas were passively emplaced and retain the fracture controlled mechanism of Pitcher (1953a) (Fig. 18B4,B5 and D).

Thus, the complete emplacement model involves ascent through a major shear zone and lateral emplacement into the wall of the shear zone.

Acknowledgments

This work was funded by doctoral programme at the University of Birmingham. Thanks to Donny Hutton for all his help and advice. The late Wally Pitcher is also thanked for his support and advice during the early stages of this work. John Reavy, Kerr Greenaway, Cathryn O'Connell and Ruth Hughes are all thanked for their assistance in the field at various stages. Charles Green and family are thanked for their hospitality during fieldwork in Dungloe. Keith Benn and Martin Feeley are thanked for insightful and constructive reviews that helped to significantly improve the manuscript. Finally, I would like to dedicate this paper to the memory of Bill Owens, without whose patient supervision AMS would have remained a mystery to me and many others. He will be sadly missed.

Appendix. Supplementary data

Supplementary data associated with this article can be found, in the online version, at doi:10.1016/j.jsg.2008.11.009.

References

Anderson, E.M., 1936. The dynamics of the formation of cone-sheets, ring-dykes and caldron-subsidence. In: Proceedings of the Royal Society of Edinburgh, vol. 56 128–157.

Berger, A.R., 1971. Dynamic analysis using dikes with oblique internal foliations. Geological Society of America Bulletin 82, 781–785.

Bouchez, J.L., 1997. Granite is never isotropic: an introduction to AMS studies of granitic rocks. In: Bouchez, J.L., Hutton, D.H.W., Stephens, W.E. (Eds.), Granite: from Segregation of Melt to Emplacement Fabrics, vol. 8. Kluwer Academic Publishers, Dordrecht, pp. 95–112.

Brun, J.P., Pons, J., 1981. Strain patterns of pluton emplacement in a crust undergoing non-coaxial deformation, Sierra-Morena, Southern Spain. Journal of Structural Geology 3, 219–229.

Bussell, M.A., Pitcher, W.S., 1985. The structural control of batholith emplacement. In: Pitcher, W.S., Atherton, M.P., Cobbing, E.J., Beckinsale, R. (Eds.), Magmatism at a Plate Edge: the Peruvian Andes. Blackie, Glasgow, pp. 167–176.

Bussell, M.A., Pitcher, W.S., Wilson, P.A., 1976. Ring complexes of Peruvian Coastal Batholith – long-standing sub-volcanic regime. Canadian Journal of Earth Sciences 13, 1020–1030.

Chernicoff, C.J., Richards, J.P., Zappettini, E.O., 2002. Crustal lineament control on magmatism and mineralization in northwestern Argentina: geological, geophysical, and remote sensing evidence. Ore Geology Reviews 21, 127–155.

Cobbing, E.J., Pitcher, W.S., 1983. Andean plutonism in Peru and its relationship to volcanism and metallogenesis at a segmented plate edge. Geological Society of America Memoirs 159, 277–291.

Cobbing, E.J., Pitcher, W.S., Wilson, J.J., Baldock, J.W., Taylor, W.P., McCourt, W., Snelling, N.J., 1981. The Geology of the Western Cordillera of Northern Peru. HMSO, London.

Cole, J.W., Milner, D.M., Spinks, K.D., 2005. Calderas and caldera structures. Earth-Science Reviews 69, 1–26.

Conliffe, J., Feely, M., 2006. Microthermometric characteristics of fluids associated with granite and greisen quartz, and vein quartz and beryl from the Rosses Granite Complex, Donegal, NW Ireland. Journal of Geochemical Exploration 89, 73–77.

Corry, C., 1988. Laccoliths: mechanisms of emplacement and growth. Geological Society of America 220, 120. Special Paper.

Cruden, A.R., 1998. On the emplacement of tabular granites. Journal of the Geological Society 155, 853–862.
Cruden, A.R., McCaffrey, K.J.W., 2001. Growth of plutons by floor subsidence: implications for rates of emplacement, intrusion spacing and melt-extraction mechanisms. Physics and Chemistry of the Earth Part A – Solid Earth and Geodesy 26, 303–315.
Dehls, J.F., Cruden, A.R., Vigneresse, J.L., 1998. Fracture control of late Archean pluton emplacement in the northern Slave Province, Canada. Journal of Structural Geology 20, 1145–1154.
Engvik, A.K., Bertram, A., Kalthoff, J.F., Stockhert, B., Austrheim, H., Elvevold, S., 2005. Magma-driven hydraulic fracturing and infiltration of fluids into the damaged host rock, an example from Dronning Maud Land, Antarctica. Journal of Structural Geology 27, 839–854.
Garza, R.A.P., Titley, S.R., Pimentel, F., 2001. Geology of the Escondida porphyry copper deposit, Antofagasta region, Chile. Economic Geology and the Bulletin of the Society of Economic Geologists 96, 307–324.
Garza-Gonzalez, C., Camprubi, A., Gonzalez-Partida, E., Arriaga-Garcia, G., Rosique-Naranjo, F., 2006. Hydrothermal alteration and fluid inclusion study of the lower cretaceous porphyry Cu–Au deposit of Tiamaro, Michoacan, Mexico. GEOFLUIDS V: 5th International Conference on Fluid Evolution, Migration and Interaction in Sedimentary Basins and Orogenic Belts. Journal of Geochemical Exploration 89, 124–128.
Guillou-Frottier, L., Burov, E., 2003. The development and fracturing of plutonic apexes: implications for porphyry ore deposits. Earth and Planetary Science Letters 214, 341–356.
Haederle, M., Atherton, M.P., 2002. Shape and intrusion style of the Coastal Batholith, Peru. Tectonophysics 345, 17–28.
Hall, A., 1966. A petrogenetic study of Rosses Granite Complex Donegal. Journal of Petrology 7, 202–220.
Halliday, A.N., Aftalion, M., Leake, B.E., 1980. A revised age for the Donegal Granites. Nature 284, 542–543.
Hutton, D.H.W., 1982. A tectonic model for the emplacement of the Main Donegal Granite, NW Ireland. Journal of the Geological Society, London 139, 615–631.
Hutton, D.H.W., 1988a. Igneous emplacement in a shear-zone termination – the biotite granite at Strontian, Scotland. Geological Society of America Bulletin 100, 1392–1399.
Hutton, D.H.W., 1988b. Granite emplacement mechanisms and tectonic controls: inferences from deformational studies. Transactions of the Royal Society of Edinburgh – Earth Sciences 79, 245–255.
Hutton, D.H.W., 1992. Granite sheeted complexes – evidence for the dyking ascent mechanism. Transactions of the Royal Society of Edinburgh – Earth Sciences 83, 377–382.
Hutton, D.H.W., 1996. The 'space problem' in the emplacement of granite. Episodes 19, 114–119.
Hutton, D.H.W., Alsop, G.I., 1996. The Caledonian strike-swing and associated lineaments in NW Ireland and adjacent areas: sedimentation, deformation and igneous intrusion patterns. Journal of the Geological Society 153, 345–360.
Hutton, D.H.W., Reavy, R.J., 1992. Strike-slip tectonics and granite petrogenesis. Tectonics 11, 960–967.
Ingram, G.M., Hutton, D.H.W., 1994. The great tonalite sill – emplacement into a contractional Shear Zone and implications for late cretaceous to early eocene tectonics in Southeastern Alaska and British Columbia. Geological Society of America Bulletin 106, 715–728.
Jacques, J.M., Reavy, R.J., 1996. Caledonian plutonism and major lineaments in the SW Scottish highlands. Journal of the Geological Society 151, 955–969.
Jelínek, V., 1978. Statistical processing of anisotropy of magnetic susceptibility measured on groups of specimens. Studia Geophysica et Geodaetica 22, 50–62.
Lacroix, S., Sawyer, E.W., Chown, E.H., 1998. Pluton emplacement within an extensional transfer zone during dextral strike-slip faulting: an example from the late Archaean Abitibi Greenstone Belt. Journal of Structural Geology 20, 43–59.
Mahan, K.H., Bartley, J.M., Coleman, D.S., Glazner, A.F., Carl, B.S., 2003. Sheeted intrusion of the synkinematic McDoogle pluton, Sierra Nevada, California. Geological Society of America Bulletin 115, 1570–1582.
McCaffrey, K.J.W., 1992. Igneous emplacement in a transpressive shear zone: Ox Mountains igneous complex. Journal of the Geological Society 149, 221–235.
McCaffrey, K.J.W., Petford, N., 1997. Are granitic intrusions scale invariant? Journal of the Geological Society 154, 1–4.
Mercy, E.L.P., 1962. The mullaghduff porphyry dyke. Transactions of the Royal Society of Edinburgh – Earth Sciences 19, 65–82.
Nicholson, R., Pollard, D.D., 1985. Dilation and linkage of echelon cracks. Journal of Structural Geology 7, 583–590.
O'Connor, P.J., Long, C.B., Keenan, P.S., Halliday, A.N., Max, M.D., Roddick, J.C., 1982. Rb–Sr isochron study of the Thorr and Main Donegal Granites, Ireland. Geological Journal 17, 279–295.
O'Driscoll, B., Stevenson, C.E., Troll, V.R., 2008. Mineral lamination development in layered gabbros of the British palaeogene igneous province: a combined anisotropy of magnetic susceptibility, quantitative textural and mineral chemistry study. Journal of Petrology 49, 1187–1221.
Owens, W.H., 1974. Mathematical model studies on factors affecting the magnetic anisotropy of deformed rocks. Tectonophysics 24, 115–131.
Owens, W.H., 1994. Laboratory drilling of field-orientated block samples. Journal of Structural Geology 16, 1719–1721.
Owens, W.H., 2000. Error estimates in the measurement of anisotropic magnetic susceptibility. Geophysical Journal International 142, 516–526.
Petford, N., Clemens, J.D., 2000. Granites are not diapiric!. Geology Today, 180–184.
Petford, N., Cruden, A.R., McCaffrey, K.J.W., Vigneresse, J.L., 2000. Granite magma formation, transport and emplacement in the earth's crust. Nature 408, 669–673.
Petronis, M.S., Hacker, D.B., Holm, D.K., Geissman, J.W., Harlan, S.S., 2004. Magmatic flow paths and palaeomagnetism of the Miocene Stoddard Mountain laccolith, iron axis region Southwestern Utah, USA. In: Martin-Hernandez, F., Luneburg, C.M., Aubourg, C., Jackson, M. (Eds.), Magnetic Fabric: Methods and Applications. Geological Society, London, Special Publications, vol. 238, pp. 251–284.
Pitcher, W.S., 1953a. The Rosses granitic ring complex, County Donegal. In: Proceedings of the Geologists' Association, vol. 64 153–182.
Pitcher, W.S., 1953b. The migmatitic older granodiorite of the Thorr District, Co. Donegal. Quarterly Journal of the Geological Society of London 108, 413–446.
Pitcher, W.S., 1997. The Nature and Origin of Granite. Chapman and Hall, London.
Pitcher, W.S., Atherton, M.P., Cobbing, E.J., Beckinsale, R., 1985. Magmatism at a Plate Edge: the Peruvian Andes. Blackie, Glasgow, pp. 328.
Pitcher, W.S., Berger, A.R., 1972. The Geology of Donegal, a Study of Granite Emplacement and Unroofing. Wiley Interscience, London.
Pitcher, W.S., Hutton, D.H.W., 2004. A Master Class Guide to the Granites of Donegal. The Geological Survey of Ireland, Dublin.
Price, A.R., 1997. Multiple Sheeting as a Mechanism of Pluton Construction: the Main Donegal Granite, NW. Ireland. Unpublished PhD thesis, University of Durham.
Read, H.H., 1958. Donegal granite. Science in Progress 182, 225–240.
Reavy, R.J., 1989. Structural controls on metamorphism and syn-tectonic magmatism – the Portuguese Hercynian collision belt. Journal of the Geological Society 146, 649–657.
Richey, J.E., 1928. Structural relations of the Mourne Granites (Northern Ireland). Quarterly Journal of the Geological Society of London 83, 653.
Richey, J.E., 1932. Tertiary ring structures in Britain. Transactions of the Geological Society of Glasgow 88, 776.
Rocchi, S., Westerman, D.S., Dini, A., Innocenti, F., Tonarini, S., 2002. Two-stage growth of laccoliths at Elba Island, Italy. Geology 30, 983–986.
Stevenson, C.T.E., Owens, W.H., Hutton, D.H.W., 2007a. Flow lobes in granite: the determination of magma flow direction in the Trawenagh Bay Granite, N.W. Ireland, using anisotropy of magnetic susceptibility. Geological Society of America Bulletin.
Stevenson, C.T.E., Owens, W.H., Hutton, D.H.W., Hood, D.N., Meighan, I.G., 2007b. Laccolithic as opposed to cauldron subsidence emplacement of the Eastern Mourne pluton, N. Ireland: evidence from anisotropy of magnetic susceptibility. Journal of the Geological Society, London 164, 99–110.
Stevenson, C.T.E., Hutton, D.H.W., Price, A.R., 2008. The Trawenagh Bay Granite and a new model for the emplacement of the Donegal Batholith. Transactions of the Royal Society of Edinburgh – Earth Sciences 97, 455–477.
Tarling, D.H., Hrouda, F., 1993. The Magnetic Anisotropy of Rocks. Chapman and Hall, New York.
Titley, S.R., Heidrick, T.L., 1978. Intrusion and fracture styles of some mineralized porphyry systems of Southwestern Pacific and their relationship to plate interactions. Economic Geology 73, 891–903.
Titley, S.R., Thompson, R.C., Haynes, F.M., Manske, S.L., Robison, L.C., White, J.L., 1986. Evolution of fractures and alteration in the Sierrita–Esperanza hydrothermal system, Pima County, Arizona. Economic Geology 81, 343–370.
Vigneresse, J.L., 2005. A new paradigm for granite generation. Transactions of the Royal Society of Edinburgh – Earth Sciences 95, 11–22.
Williams, W.C., Meissl, E., Madrid, J., de Machuca, B.C., 1999. The San Jorge porphyry copper deposit, Mendoza, Argentina: a combination of orthomagmatic and hydrothermal mineralization. Ore Geology Reviews 14, 185–201.
Young, D.G.G., 1974. Donegal granite – gravity analysis. In: Proceedings of the Royal Irish Academy Section B-Biological Geological and Chemical Science, vol. 74 63–73.